IEEE Transactions on Wireless Communications

Fine-over-Coarse Spectrum Sharing with Shaped Virtual Cells for Hybrid Satellite-UAV-Terrestrial Maritime Networks

Journal:	*IEEE Transactions on Wireless Communications*
Manuscript ID	Paper-TW-Apr-24-0683.R1
Manuscript Type:	Original Transactions Paper (S1)
Date Submitted by the Author:	02-Jul-2024
Complete List of Authors:	Wang, Yanmin; Minzu University of China, School of Information Engineering Feng, Wei; Tsinghua University, Electronic Engineering Wang, Jue; Singapore University of Technology and Design (SUTD), ; Nantong University, School of Electronic and Information Engineering Zhou, Shidong; Tsinghua University, Electronic Department; Wang, Cheng-Xiang; Southeast University, National Mobile Communications Research Laboratory; Purple Mountain Laboratories, Pervasive Communication Research Center
Keyword:	

Response to Reviewers' Comments

Paper-TW-Apr-24-0683

We first sincerely thank the Editor and the Reviewers for their generous devotions and insightful comments to the paper, which have helped us improve the quality of the paper greatly. The paper has been revised and enriched per the Editor's and the Reviewers' comments and suggestions. Also, a point-by-point response to the comments has been made.

Editor,

Thank you so much for your devotions to the reviewing of our paper. The insightful and inspiring comments and suggestions from you and the reviewers have been carefully considered and seriously discussed. Per your and the reviewers' comments and suggestions, our main revisions are summarized as follows.

The system model has been enriched to address the concerns of you, the editor, and the reviewers. Specifically, the acquisition of the global knowledge for spectrum sharing, which mainly includes the large-scale CSI of the links and the QoS requirements of the vessel users, in the central controller, is addressed. The impact of the mobility of the satellite, the UAVs and the vessels on spectrum sharing, as well as the measure to deal with the variation of the large-scale CSI, have been illustrated. The role of time slices in the proposed spectrum sharing framework, and the relation between time slices and time slots, are explained. The role of fine time synchronization and that of coarse time synchronization are clarified.

Further, the illustrations on the proposed spectrum sharing framework and scheme are revised, to elaborate how the fine-over-coarse mechanism works. The role of shaped virtual cells in spectrum sharing is also emphasized. Besides, the reason for the performance gain of the proposed spectrum sharing scheme compared to the Random I/II scheme is explained in the simulation part.

We have carefully considered and seriously responded to the comments and suggestions, especially the following concerns, via the revisions in the paper.

- **How to obtain global knowledge for the central controller?** To address this

concern, we have added "Global knowledge of the MCN that is needed for spectrum sharing, including CSI of the links and QoS requirements of the vessel users, could be obtained via the signaling channels provided by the satellite" at the end of the first paragraph of Section II-A, on Page 3, and "The acquisition of large-scale CSI could be accomplished via either centralized calculation based on the large-scale fading models, e.g., (2)-(4), or in a more precise way via distributed link-by-link estimation" in the last paragraph of Section II-A, on Page 4.

- **The mobility of satellites and UAVs is not considered.** As only large-scale CSI is utilized in the proposed spectrum sharing framework and scheme, the impact of the mobility of the satellite, the UAVs and the vessels mainly focuses on the variation of the large-scale CSI of the links. To remove the ambiguity, it is pointed out that "Due to the mobility of the UAVs, vessels, as well as the satellite, the transmission distances, i.e., $d_{n_1}^{(s,v)}$, $d_{n_2}^{(v,u)}$, $d_{n_2}^{(v,v)}$ and $d_{n_2,n_1}^{(v,v)}$, and correspondingly the large-scale CSI for the links, may vary slightly during the serving time T. Accordingly, average large-scale CSI could be utilized for spectrum sharing in T" at the end of the last paragraph of Section II-A, on Page 4.
- **How to acquire large-scale CSI?** To be clearer, it is emphasized that "Global knowledge of the MCN that is needed for spectrum sharing, including CSI of the links and QoS requirements of the vessel users, could be obtained via the signaling channels provided by the satellite" at the end of the first paragraph in Section II-A, on Page 3, and that "The acquisition of large-scale CSI could be accomplished via either centralized calculation based on the large-scale fading models, e.g., (2)-(4), or in a more precise way via distributed link-by-link estimation" in the last paragraph of Section II-A, on Page 4.
- **How to address CSI variation?** For this concern, we have added "Due to the mobility of the UAVs, vessels, as well as the satellite, the transmission distances, i.e., $d_{n_1}^{(s,v)}$, $d_{n_2}^{(v,u)}$, $d_{n_2}^{(v,v)}$ and $d_{n_2,n_1}^{(v,v)}$, and correspondingly the large-scale CSI for

the links, may vary slightly during the serving time T. Accordingly, average large-scale CSI could be utilized for spectrum sharing in T" at the end of the last paragraph of Section II-A, on Page 4.

- **The novelty of time slices.** Actually, time slices are introduced for convenience to represent the total serving time allocated to the vessel users for QoS guarantees. To remove the ambiguity on this point, a footnote is added for further explanation on time slicing in the second paragraph of Section II-A, on Page 3. That is "In practical applications, time slots with the same duration can be utilized, and uneven time slicing could be achieved by uneven allocation of time slots", which appears at the bottom of the right column on Page 3.
- **Fine synchronization is not used.** To be clearer, we have revised and enriched the illustrations on fine and coarse time synchronization. Specially, it is emphasized at the end of the second paragraph in Section II-A, on Pages 3-4, that "To circumvent the challenge of fine-grained network-wide time synchronization, it is assumed that time-slice-oriented fine synchronization is only achieved locally and separately among the V2S links and among the U2V and V2V links. The scheduling of the V2S links and that of the U2V and V2V links are only coarsely synchronized at the time scale T. That is only coarse time synchronization at the time scale T, which could be much larger than the duration of a single time slice, is achieved across the MCN for spectrum sharing between the V2S links and the U2V and V2V links".

We hope that these revisions adequately address the concerns corresponding to the comments and suggestions. Looking forward to the editorial team's feedback! Thank you again for your generous devotions to the reviewing of our paper and the precious opportunity for us to improve the quality of our work!

Response to Reviewer 1

We sincerely thank the reviewer for his/her detailed comments and beneficial suggestions, as well as the generous recognition for our work. The response to the reviewer's specific comments and the corresponding modifications to the paper are as follows.

Comment 1: *According to the illustration in the paper, the implementation of the proposed spectrum sharing scheme needs centralized computation and control in the central controller. How does the central controller obtain the global knowledge of the MCN that is necessary for spectrum sharing?*

Response: Thanks for raising this point. The global knowledge of the MCN that is needed for spectrum sharing mainly includes the large-scale CSI of the links and the QoS requirements of the vessel users. The central controller can obtain the global knowledge of the MCN via the signaling channels provided by the satellite.

To be clearer, the description of the system model in Section II-A is enriched. It is specifically pointed out that "Global knowledge of the MCN that is needed for spectrum sharing, including CSI of the links and QoS requirements of the vessel users, could be obtained via the signaling channels provided by the satellite" at the end of the first paragraph of Section II-A, on Page 3. Further, for the acquisition of the large-scale CSI, we have added that "The acquisition of large-scale CSI could be accomplished via either centralized calculation based on the large-scale fading models, e.g., (2)-(4), or in a more precise way via distributed link-by-link estimation" in the last paragraph of Section II-A, on Page 4.

Comment 2: *Is the satellite in the MCN deployed in GEO or LEO? For the latter, the mobility of the satellite must be considered. Also, the mobility of the UAVs and vessels should also be considered. What is the impact of the mobility of the satellite, UAVs, and*

vessels on the proposed spectrum sharing scheme?

Response: It is rather appreciated that you have raised this insightful point. The paper puts no special constraints on the type of the satellite in the MCN. It can be deployed in either GEO or LEO. In the simulations presented in Section IV, an LEO satellite is considered, which is supposed to be deployed in an orbit with an altitude of 1000km. Due to the mobility of the satellite, UAVs, and vessels, the transmission distances and further the large-scale CSI for the links may vary slightly during the serving time T. A simple and straightforward way to take the impact of the mobility into consideration is to utilize the average large-scale CSI within the serving time T in spectrum sharing optimization. To achieve higher accuracy, more complex measures may be adopted alternatively, which we will consider delicately in our future work.

Following the reviewer's comment and suggestions, we have added some explanation on this point in the revised paper. Specifically, we have emphasized that "Due to the mobility of the UAVs, vessels, as well as the satellite, the transmission distances, i.e., $d_{n_1}^{(s,v)}$, $d_{n_2}^{(v,u)}$, $d_{n_2}^{(v,v)}$and $d_{n_2,n_1}^{(v,v)}$, and correspondingly the large-scale CSI for the links, may vary slightly during the serving time T. Accordingly, average large-scale CSI could be utilized for spectrum sharing in T" at the end of the last paragraph of Section II-A, on Page 4.

Comment 3: *It is supposed that the time slicing in each subcarrier could be even or uneven. In practical communication networks, time slots with the same duration are usually adopted. Why is uneven time slicing assumed?*

Response: Thank you for this comment. Uneven time slicing is adopted in the paper for serving time allocation among the vessel users for QoS guarantees. The duration of a time slice represents the total serving time allocated to a certain vessel user in a certain subcarrier. In practical applications, uneven time slicing may be achieved in different ways. Specially, time slots with the same duration can be utilized, and uneven time slicing could be achieved by uneven allocation of time slots.

To remove the ambiguity on this point, a footnote is added for further explanation on uneven time slicing in the second paragraph of Section II-A, on Page 3. That is "In practical applications, time slots with the same duration can be utilized, and uneven time slicing could be achieved by uneven allocation of time slots", which appears at the bottom of the right column on Page 3.

Comment 4: *What is the role of shaped virtual cells in the proposed spectrum sharing scheme? What does "shaped" mean?*

Response: Thank you for this inspiring comment. As a matter of fact, shaped virtual cells constitute the basis for the proposed fine-over-coarse spectrum sharing scheme. In the proposed scheme, the V2S links for the vessels in the same shaped virtual cell form a V2S link cluster, and are scheduled in one subcarrier exclusively. With shaped virtual cells, successive time slices of each subcarrier could be grouped together and allocated as a whole to a V2S link cluster. Accordingly, fine-grained time synchronization at the scale of single time slices could be circumvented. By "shaped", we refer to the principle for the formation of the virtual cells and the clustering of the V2S links.

Inspired by this comment, we have enriched the related illustrations in the second paragraph of Section III-B, in the right column of page 6 and the left column of Page 7, as "the V2S links that may cause similar interference to the U2V and V2V links should be grouped together, so that the diversity of the V2S links in inter-link interference could be reserved and opportunistically utilized for spectrum sharing" and "Besides, it is noted that the impact of inter-link interference is closely coupled with the geographical distribution, as well as QoS requirements, of the vessels n_1 and n_2. Thus, clustering of the V2S links can be seen as forming K *virtual cells* for the vessels n_1 in the large coverage area of the satellite, *shaped* by the distribution and QoS requirements of all vessel users. Each *shaped virtual cell* is allocated one subcarrier exclusively, and the U2V and V2V links for the vessels n_2 share the subcarriers opportunistically, based on the profile of the interference caused by the V2S links in

each virtual cell". Furthermore, the role of shaped virtual cells is emphasized in the introduction part, by adding "Specially, shaped virtual cells are formed within the large coverage area of the satellite, and V2S links for vessel users in the same virtual cell form a V2S link cluster", in the middle of the first paragraph on Page 2.

Comment 5: *It is said that "A single V2S link is allowed to belong to different V2S link clusters simultaneously, and a subcarrier may also be allocated to more than one V2S link clusters" with the formulated problem. However, it is shown in Fig. 2 that each V2S link belongs to only one link cluster. Besides, each subcarrier is allocated to only one V2S link cluster in the proposed scheme. Why does that happen?*

Response: Thank you for the detailed and profound comment. Just as you have pointed out, in the problem formulation given by (11), the mapping between the V2S links and the V2S link clusters is not restricted so as to reserve as much flexibility as possible. Nevertheless, Theorem 1 presented in Section III-A, in the left column of Page 6, indicates that when the formulated problem is feasible and the MCN is full-loaded, i.e, "$\lceil(\sum_{n_1=1}^{N_1} V_{n_1}^{QoS}/R_{n_1})/T\rceil = K'$" and "$K' = K$", there must be an optimal solution in which each subcarrier is allocated to only one V2S link cluster, i.e., "$\sum_{c=1}^{C_{V2S}^*} \eta_{k,c}^* = 1$". The proposed scheme is derived following Theorem 1. Thus, each subcarrier is allocated to only one V2S link cluster in the proposed scheme.

Fig. 2 shows the shaped virtual cells formed for the MCN considered in the simulations in Section IV. In the MCN considered in Section IV, the QoS requirement of each vessel n_1 is set to be proportional to the transmission rate of the V2S link that serves it, i.e., "$V_{n_1}^{QoS} = (KT/N_1)\mathcal{R}_{n_1}$". Correspondingly, when only the QoS requirements of the vessels n_1 are concerned, the N_1 vessels could be grouped into K shaped virtual cells randomly, as long as with N_1/K vessels in each cell. Following the steps in the proposed scheme, K such shaped virtual cells are delicately formed by grouping the vessels n_1 that cause similar inter-link interference together, taking the QoS requirements of all the vessels n_1 and n_2 into consideration. That is why each V2S link belongs to only one link cluster in Fig. 2. It is worth noting that generally speaking, a V2S link may

belong to multiple link clusters simultaneously in the proposed scheme.

Comment 6: *It can be seen from Figs.5-7 and Fig. 8(b)-(d) that the energy saving of the proposed scheme compared to the Random-II scheme is close to100%. Why is that?*

Response: Thank you for this comment. The Random-II scheme is a completely random scheme with both random clustering, of the V2S links, and random scheduling, of the U2V and V2V links. With the Random-II scheme, the U2V and V2V links tend to suffer from severe inter-link interference caused by the V2S links. Consequently, much more energy is needed to guarantee the QoS requirements of the vessel users.

To explain the mentioned phenomenon in the simulation results, we have added "Specially, Figs. 5-7 and Fig. 8(b)-(d) show that the proposed scheme saves more than 90% of the energy compared to the Random-II scheme. The reason is that severe inter-link interference tends to happen with both random V2S link clustering and U2V/V2V link scheduling. Accordingly, much more energy is needed to guarantee the QoS requirements of the vessel users for the Random-II scheme", in the first paragraph of the right column on Page 11.

Comment 7: *A typo happens in the sentence "For efficient calculation of R_{n1} and R_{n2,k} given by (5b) and (9) during the execution of Algorithm 2". "(5b)" should be "5(a)", as R_{n1} is given by 5(a) instead of (5b).*

Response: Thank you for the devotions to the careful reading of our paper. The typo has been corrected in the revised paper. Further, we have carefully read through the whole paper to check whether other typos exist.

Again, thank you so much for all the insightful comments, helpful suggestions, as well as the devotions to the reviewing of our paper!

Response to Reviewer 2

We sincerely thank the reviewer for his/her insightful comments and helpful suggestions. Also, gratefulness is expressed here for the positive evaluation of the paper. In the following, the reviewer's specific comments are responded, and the modifications to the paper are illustrated.

Comment 1: *For saving cost, only large-scale CSI is adopted in the proposed spectrum sharing scheme. Due to the mobility of the UAVs and vessels, as well as that of the satellite when it is deployed in LEO, the path loss of the links may vary within the serving time T in the MCN. How to deal with the variation of path loss in the acquisition of the large-scale CSI for the links?*

Response: It is rather appreciated that the reviewer has raised this insightful point. In the hybrid MCN considered in the paper, the large-scale fading of the links is mainly caused by path loss. Indeed, due to the mobility of the UAVs and vessels, as well as that of the satellite when it is deployed in LEO, the transmission distances and further the path loss of the links may vary slightly during the serving time T. A simple and straightforward way to take the impact of the mobility into consideration is to utilize the average path loss, i.e., average large-scale CSI, within the serving time T in spectrum sharing optimization. To achieve higher accuracy, more complex measures may be adopted alternatively, which we will consider delicately in our future work.

Following the reviewer's comment, we have added some explanation on this point in the revised paper. Specifically, it is emphasized that "Due to the mobility of the UAVs, vessels, as well as the satellite, the transmission distances, i.e., $d_{n_1}^{(s,v)}$, $d_{n_2}^{(v,u)}$, $d_{n_2}^{(v,v)}$and $d_{n_2,n_1}^{(v,v)}$, and correspondingly the large-scale CSI for the links, may vary slightly during the serving time T. Accordingly, average large-scale CSI could be utilized for spectrum sharing in T" at the end of the last paragraph in Section II-A, on Page 4.

Comment 2: *Time slicing is adopted together with subcarrier division in the paper for*

efficient spectrum utilization. It is said that "The time slicing in each subcarrier could be even or uneven, according to the QoS requirements of the vessels". Uneven time slicing could complicate time synchronization and is usually not adopted in practical networks. Please clarify the reason for uneven time slicing.

Response: Thank you for this detailed and inspiring comment. In the paper, uneven time slicing is utilized for serving time allocation among the vessel users for QoS guarantees. The duration of a time slice represents the total serving time allocated to a certain vessel user in a certain subcarrier. In practical applications, uneven time slicing may be achieved in different ways. Specially, when time slots with the same duration are adopted, uneven time slicing could be achieved via uneven allocation of time slots.

To remove the ambiguity on uneven time slicing, a footnote is added for further explanation in the second paragraph of Section II-A, on Page 3. That is "In practical applications, time slots with the same duration can be utilized, and uneven time slicing could be achieved by uneven allocation of time slots", which appears at the bottom of the right column on Page 3.

Comment 3: *As a prerequisite for the proposed spectrum sharing scheme, it is assumed that the MCN is in a full-load state. Accordingly, C_{V2S} = K V2S links clusters are formed based on the analysis on the optimal solution for the formulated spectrum sharing problem. Is the proposed scheme effective when the MCN is not totally fully loaded?*

Response: Thank you for this comment. It is believed that after some adaptive modifications, the proposed spectrum sharing scheme may also be utilized when the MCN is not totally fully loaded.

As a prerequisite for the proposed scheme, it is assumed that the MCN is in a full-load state with respect to the vessels served by V2S links, i.e., "$(\sum_{n_1=1}^{N_1} V_{n_1}^{QoS}/R_{n_1})/T = K$". When the MCN is not fully loaded, we suppose that the serving time of a duration $\hat{T}$,

$0 < \hat{T} < T$, with K subcarriers, or $\hat{K}$, $0 < \hat{K} < K$, subcarriers with the serving time T, is/are enough to satisfy the QoS requirements of the vessels served by V2S links. Accordingly, the proposed scheme could be utilized for spectrum sharing between the V2S and U2V/V2V links in the serving time $\hat{T}$ and K subcarriers, or in the serving time T and $\hat{K}$ subcarriers. The left serving time $T - \hat{T}$ in K subcarriers, or the left $K - \hat{K}$ subcarriers in the serving time T, can be allocated exclusively to the U2V and V2V links, with no inter-link interference from the V2S links. It can be inferred that with the above modifications, the proposed scheme could still be effective for the MCN when it is not fully loaded.

Considering that the assumption that the MCN is in a full-load state is more consistent with the background that spectrum sharing is needed between the links, the proposed scheme in the revised paper still targets at MCNs that are fully loaded. Nevertheless, we will keep the comment in mind and give it special attention in our future work.

Comment 4: *In the hybrid MCN, backhaul links are usually needed by the UAVs and the vessels acting as hot spots. Can the backhaul links be included in the proposed spectrum sharing framework?*

Response: Thank you for this inspiring comment. It inspires us to make more comprehensive considerations on how to put the proposed spectrum sharing framework into practical applications. In the design and operation of a practical MCN, it is crucial to consider all related links, including the backhaul links for the UAVs and the vessels acting as hot spots.

The answer to the question in the comment is yes and no. Backhaul links for the UAVs and the vessels acting as hot spots could be established via the satellite in the hybrid MCN. Accordingly, the uplink parts of the backhaul links could be considered in a similar way as the V2S links in the proposed spectrum sharing framework. As to the downlink parts of the backhaul links, they are different from the links involved in the proposed framework, and need to be considered independently. To be concise and to

focus on the most typical links, we haven't taken the backhaul links into consideration in the revised paper. Alternatively, we will keep it in mind and give it enough attention when we take a step further in the future.

Again, thank you so much for all the insightful comments, helpful suggestions, as well as the devotions to the reviewing of our paper!

Response to Reviewer 3

We sincerely thank the reviewer for his/her inspiring comments and beneficial suggestions. Also, thanks so much for the generous recognition for our work. In the following, the reviewer's specific comments are responded, and the modifications to the paper are illustrated.

Comment 1: *Large-scale CSI is utilized in the proposed spectrum sharing scheme. How to acquire the large-scale CSI of the links in the hybrid MCN?*

Response: Thank you for this inspiring comment. The acquisition of the large-scale CSI could be accomplished via either centralized calculation based on the large-scale fading models, e.g., (2)-(4), or in a more precise way via distributed link-by-link estimation, with the help of the signaling channels provided by the satellite.

To be clearer, the description of the system model in Section II-A is enriched. It is specifically pointed out that "Global knowledge of the MCN that is needed for spectrum sharing, including CSI of the links and QoS requirements of the vessel users, could be obtained via the signaling channels provided by the satellite" at the end of the first paragraph in Section II-A, on Page 3. Further, we have added that "The acquisition of large-scale CSI could be accomplished via either centralized calculation based on the large-scale fading models, e.g., (2)-(4), or in a more precise way via distributed link-by-link estimation" in the last paragraph of Section II-A, on Page 4.

Comment 2: *Time slices instead of time slots are utilized in the paper. What is the uniqueness of time slices in the paper?*

Response: Thank you for raising this point. Time slicing is adopted in the paper for serving time allocation among the vessel users for QoS guarantees. The duration of a time slice represents the total serving time allocated to a certain vessel user in a certain

subcarrier. According to the QoS requirements of the vessel users, time slicing in each subcarrier could be even or uneven.

As for uneven time slicing, it can be achieved in different ways in practical applications. Specially, time slots with the same duration can be utilized, and uneven time slicing could be achieved by uneven allocation of time slots. To be clearer, a footnote is added for further explanation on uneven time slicing in the second paragraph of Section II-A, on Page 3. That is "In practical applications, time slots with the same duration can be utilized, and uneven time slicing could be achieved by uneven allocation of time slots", which appears at the bottom of the right column on Page 3.

Comment 3: *In the proposed spectrum sharing scheme, only coarse time synchronization across the network is assumed. As time slicing is implemented in the subcarriers, time-slice-based fine synchronization should also be needed for link scheduling. How does the fine-over-coarse mechanism work in spectrum sharing?*

Response: Thank you for this comment. Indeed, time-slice-based fine synchronization is needed for both the scheduling of the V2S links and that of the U2V and V2V links in the time slices. In the proposed spectrum sharing framework and scheme, such fine time synchronization only needs to be achieved respectively among the V2S links and among the U2V/V2V links. It is not needed between any V2S link and U2V/V2V link for spectrum sharing. Instead, only coarse time synchronization is needed between the V2S links and the U2V/V2V links to implement spectrum sharing optimization.

To be clearer, we have revised and enriched the illustrations on fine and coarse time synchronization in the paper. Specially, it is emphasized at the end of the second paragraph in Section II-A, on Pages 3-4, that "To circumvent the challenge of fine-grained network-wide time synchronization, it is assumed that time-slice-oriented fine synchronization is only achieved locally and separately among the V2S links and among the U2V and V2V links. The scheduling of the V2S links and that of the U2V and V2V links are only coarsely synchronized at the time scale T. That is only coarse

time synchronization at the time scale T, which could be much larger than the duration of a single time slice, is achieved across the MCN for spectrum sharing between the V2S links and the U2V and V2V links". In addition to this, the fine-over-coarse mechanism in the proposed spectrum sharing framework and scheme is illustrated in several parts of the paper. Specially, in the third paragraph of Section I, on Page 2, we have "the V2S links are dynamically grouped into *clusters* according to the impact of inter-link interference, and then jointly scheduled with U2V and V2V links in terms of *link clusters*" and "Specially, shaped virtual cells are formed within the large coverage area of the satellite, and V2S links for vessel users in the same virtual cell form a V2S link cluster. By V2S-link-cluster-based scheduling, successive time slices of each subcarrier could be grouped together and assigned adaptively to each of the V2S link clusters as a whole". In the second paragraph of Section III-B, in the right column on Page 6 and the left column on Page 7, it is pointed out that "the V2S links that may cause similar interference to the U2V and V2V links should be grouped together, so that the diversity of the V2S links in inter-link interference could be reserved and opportunistically utilized for spectrum sharing" and "clustering of the V2S links can be seen as forming K *virtual cells* for the vessels n_1 in the large coverage area of the satellite, *shaped* by the distribution and QoS requirements of vessel users. Each *shaped virtual cell* is allocated one subcarrier exclusively, and the U2V and V2V links for the vessels n_2 share the subcarriers opportunistically, based on the profile of the interference caused by the V2S links in each virtual cell".

Comment 4: *Spectrum reuse is only implemented between V2S links and U2V/V2V links in the proposed scheme. When distances between U2V/V2V links are large enough, spectrum reuse may also be implemented among them. Will the proposed spectrum sharing framework work when spectrum reuse between U2V/V2V links is adopted?*

Response: Thank you for raising this insightful point. It actually can help us extend the application scenarios of the proposed spectrum sharing framework. It is believed that the proposed framework will still work when spectrum reuse between U2V/V2V links is adopted, after some adaptive modifications.

Based on the illustrations in Algorithm 2, on Page 9, it can be inferred that if the scheduling of the U2V and V2V links in Step 4 is adaptively modified, the proposed spectrum sharing scheme can be applied to the scenario where spectrum reuse between U2V/V2V links is also adopted. More specifically, the inter-link interference between U2V/V2V links should be taken into consideration in the scheduling optimization in Step 4 of Algorithm 2. Accordingly, non-convex optimization methods may need to be utilized to deal with the inter-link interference among U2V/V2V links, instead of just solving the linear programming problem in (18). While noting this possible extension of the proposed spectrum sharing framework, in order to be concise and to focus on the main target, we haven't taken the spectrum reuse between U2V/V2V links into consideration in the revised paper. Nevertheless, we will keep it in mind and give it special attention in our future work.

Comment 5: *It is observed from Figs.5-7 that a huge difference exists between the energy consumption achieved by the proposed scheme and that by the Random-I/II scheme. Why is that?*

Response: Thank you for this detailed and inspiring comment. The Random-I scheme is obtained based on random clustering of the V2S links and optimal scheduling of the U2V and V2V links via Theorem 1. The Random-II scheme is a completely random scheme with both random clustering, of the V2S links, and random scheduling, of the U2V and V2V links. When the Random-I or Random-II scheme, especially the Random II scheme, is implemented, the U2V and V2V links tend to suffer from severe inter-link interference caused by the V2S links. Consequently, much more energy is needed to guarantee the QoS requirements of the vessel users.

To explain the huge difference between the performance of the proposed scheme and that of the Random-I/II scheme, especially the Random II scheme, we have added "Specially, Figs. 5-7 and Fig. 8(b)-(d) show that the proposed scheme saves more than 90% of the energy compared to the Random-II scheme. The reason is that severe inter-

link interference tends to happen with both random V2S link clustering and U2V/V2V link scheduling. Accordingly, much more energy is needed to guarantee the QoS requirements of the vessel users for the Random-II scheme", in the first paragraph of the right column on Page 11.

Again, thank you so much for all the inspiring comments, beneficial suggestions, as well as the devotions to the reviewing of our paper!

Fine-over-Coarse Spectrum Sharing with Shaped Virtual Cells for Hybrid Satellite-UAV-Terrestrial Maritime Networks

Yanmin Wang, Wei Feng, *Senior Member, IEEE*, Jue Wang, *Member, IEEE*,
Shidong Zhou, and Cheng-Xiang Wang, *Fellow, IEEE*

***Abstract*—Spectrum sharing among the satellite, unmanned aerial vehicle (UAV), and terrestrial components is crucial to alleviate spectrum scarcity in a hybrid maritime communication network (MCN). Fine-grained spectrum sharing based on *ms*-level time-domain slices is widely envisioned. However, *ms*-level time synchronization is challenging in the hybrid MCN due to the large diversity in the link delay. To tackle this challenge, we propose a *fine-over-coarse* spectrum sharing framework based on coordinated link scheduling, which is realized by joint subcarrier and time slice allocation. Specially, by link-cluster-based scheduling with grouped time slice allocation for the satellite links, time-slice-oriented spectrum sharing is realized with coarse time synchronization at time scales much larger than a single time slice duration. In the framework, only large-scale channel state information (CSI) is utilized for saving cost. A *worst-case* model is introduced to depict interference caused by satellite link clusters, and an NP-hard mixed integer programming (MIP) problem is formulated. Based on analysis on the characteristics of the optimal solution, a novel link clustering algorithm is proposed to form a group of shaped virtual cells within the coverage area of the MCN. A suboptimal spectrum sharing scheme with only a small performance gap to the optimal one is then proposed. Simulations show that a significant improvement in both energy efficiency and spectrum efficiency can be achieved by the proposed framework.**

***Index Terms*—Maritime communication, hybrid network, spectrum sharing, time synchronization, channel state information (CSI)**

I. Introduction

Ubiquitous coverage is ranked among the top targets of the sixth generation (6G) network, for which enhanced maritime coverage is considered to be a key scenario [1]–[4]. Since the terrestrial base stations (BSs), in general, are only suitable for off-shore coverage, the non-terrestrial network components, including satellites and unmanned aerial vehicles (UAVs), are indispensable for realizing broadband maritime communications in a wide area [1], [3]–[9]. With the ability to integrate the advantages of different networks together, the hybrid satellite-UAV-terrestrial network is considered to be a promising solution for 6G maritime coverage [10]–[14]. Specially, satellites, UAVs, as well as vessels with spare communication capability, could all act as access points to serve maritime users on demand. To counter spectrum scarcity and fully exploit the potential gains of a hybrid satellite-UAV-terrestrial maritime communication network (MCN), efficient spectrum sharing among all the involved communication links is necessary [2]–[4], [11], [13], [15].

In a hybrid satellite-UAV-terrestrial MCN, the vessel users are usually dispersively distributed in a large area, especially those served by satellite beams [8], [12]–[14]. Accordingly, the communication links to different users are largely different in the propagation delay and path loss [8]. The most prominent difference happens between satellite links and UAV and terrestrial links. Due to the high altitude of satellites, the propagation delay and path loss suffered by satellite links are much larger than those by UAV and terrestrial links. This brings both opportunities and challenges for spectrum sharing. On one hand, the diversity in the path loss of the links, including both the communication links and interference links, brings extra chances for opportunistic spectrum utilization [8], [13], [16]. On the other hand, the difference in the propagation delay of different links makes it difficult to achieve fine-grained time synchronization across the hybrid MCN, especially when the satellite, UAV, and terrestrial components are operated separately with limited information exchange. Thus, when time slicing is adopted together with subcarrier division for the spectrum utilization,[1] it will be rather challenging to implement cooperative spectrum sharing optimization in the hybrid MCN [7], [8], [17]–[19]. Further, the large propagation delay of satellite links makes it difficult to obtain perfect instantaneous channel state information (CSI) for spectrum sharing optimization [16], [25]–[27].

In this paper, *fine-over-coarse* spectrum sharing is explored for a hybrid satellite-UAV-terrestrial MCN, where UAV-to-vessel (U2V) and vessel-to-vessel (V2V) links reuse the same frequency band with vessel-to-satellite (V2S) links. With spectrum resource being utilized in terms of time-sliced subcarri-

Yanmin Wang is with the School of Information Engineering, Minzu University of China, Beijing 100081, China (email: wangyanmin@muc.edu.cn).

Wei Feng is with the Department of Electronic Engineering, Tsinghua University, Beijing 100084, China (email: fengwei@tsinghua.edu.cn).

Jue Wang is with the School of Information Science and Technology, Nantong University, Nantong 226019, China, and also with the Nantong Research Institute for Advanced Communication Technology, Nantong 226019, China (email: wangjue@ntu.edu.cn).

Shidong Zhou is with the Department of Electronic Engineering, Tsinghua University, Beijing 100084, China (email: zhousd@tsinghua.edu.cn).

Cheng-Xiang Wang is with National Mobile Communications Research Laboratory, School of Information Science and Engineering, Southeast University, Nanjing 210096, China, and also with Purple Mountain Laboratories, Nanjing 211111, China (email: chxwang@seu.edu.cn).

[1]As a basic spectrum utilization scheme designed based on time division multiple access (TDMA) and frequency division multiple access (FDMA) for satellite communications, multi-frequency-TDMA (MF-TDMA) is proved to be rather flexible in practical applications [17].

ers, link scheduling is implemented based on subcarrier and time slice allocation. To circumvent challenges brought by network-wide fine-grained time synchronization, the V2S links are dynamically grouped into *clusters* according to the impact of inter-link interference, and then jointly scheduled with U2V and V2V links in terms of *link clusters* instead of individual links. Specially, shaped virtual cells are formed within the large coverage area of the satellite, and V2S links for vessel users in the same virtual cell form a V2S link cluster. By V2S-link-cluster-based scheduling, successive time slices of each subcarrier could be grouped together and assigned adaptively to each of the V2S link clusters as a whole. With delicately-designed V2S link clusters, fine-grained time-slice-oriented coordination between V2S links and U2V and V2V links in joint link scheduling could be achieved with coarse time synchronization at time scales much larger than single time slices. Besides, only large-scale CSI of the links is utilized. As compared to instantaneous CSI which is fast varying, large-scale CSI usually varies much more slowly and is less sensitive to delay. Also, the acquisition of large-scale CSI incurs a much reduced overhead and signaling cost, and is more friendly to practical applications [12]–[14], [16], [24]. By implementing link-cluster-based spectrum sharing optimization with the aid of large-scale CSI, a practical-application-friendly spectrum sharing scheme is anticipated to be derived for the MCN.

A. Related Works

1) Hybrid satellite, UAV, and terrestrial MCNs: Maritime communications have been attracting ever-increasing research attentions due to the importance of blue economy [4]–[6], [12]–[14]. Satellite communications, established via either geosynchronous orbit (GSO) or low earth orbit (LEO) satellites, have been big hits for maritime coverage, especially for remote areas far off the shore [1]–[4], [7], [8]. While the satellite solution can provide wide-area coverage and geographical-location-independent access, it suffers from inherent drawbacks such as large path loss and high cost for high-speed transmissions. To provide cost-efficient broadband maritime coverage, researchers have turned to terrestrial and airborne MCNs relying on vessels and UAVs as relays [5], [6]. Compared to the access through satellites, the V2V and U2V links are more efficient alternatives for maritime users to achieve high-speed transmission, thanks to the much shorter propagation distances and much lower implementation cost. Further, the hybrid satellite-UAV-terrestrial MCN has been investigated as an integrated solution [8], [12]–[14]. It is demonstrated that by effectively integrating the satellites, the UAVs, and the vessels together, the hybrid satellite-UAV-terrestrial MCN promises an optimistic prospect for cost-effective on-demand maritime coverage [8], [12]–[14].

2) Spectrum sharing in hybrid networks: Although new spectrums have been continuously explored and utilized, spectrum scarcity is still a big challenge that has to be coped with delicately [1]–[4]. A widely-recognized countermeasure for spectrum scarcity is cooperative spectrum sharing between different components of a hybrid network [20]–[23]. Under constraints on interference caused to incumbent terrestrial networks, resource allocation, including the beam, power, and channel resources, was optimized for cognitive satellite downlinks and uplinks in the Ka band in [20]. In [21], the outage probability was derived for a hybrid satellite-terrestrial spectrum sharing system, where multiple terrestrial transmitter-receiver pairs cooperate with a primary satellite network for dynamic spectrum access. A joint beamforming and power allocation scheme was proposed in [22] to maximize the sum rate of satellite-terrestrial integrated networks, where the satellite multicast downlinks and the terrestrial downlinks serving a group of non-orthogonal multiple access (NOMA) users share the same mmWave frequency band. In [23], with the presence of a primary satellite-receiver link, multiple UAVs with aerial stations and a terrestrial BS were deployed to support smart vehicles, and user association, power optimization, and trajectory control were jointly optimized. With the assumption that perfect instantaneous CSI was available for all the links, spectrum sharing in [20]–[23] was mainly achieved through opportunistic coordination between satellite and UAV/terrestrial links in the frequency domain, either with or without subcarrier division. Opportunistic optimization in the time domain, e.g., across time slots, was either not considered or just considered for the UAV/terrestrial links [20]–[23]. For example, although opportunistic optimization based on time slots was considered in [23], it was only for the UAV and terrestrial links, and a single satellite link was supposed to occupy the frequency band statically across all time slots.

3) Large-scale CSI vs. instantaneous CSI: While a lot of inspiring results have been achieved on spectrum sharing for hybrid networks in [20]–[23], the acquisition of the instantaneous CSI is rather challenging, or even impossible in some cases, due to the costly overhead and the large propagation delay of the links between satellites and maritime users. To tackle the challenge, spectrum sharing based on large-scale CSI has been proposed [16], [25]–[27]. With only the information of path loss and shadowing obtained from a pre-constructed radio map, power allocation and user scheduling schemes were proposed for a hybrid satellite-terrestrial network in [16]. A general problem of resource scheduling for spectrum sharing was discussed in [25], for a typical case where mobile wireless and meteorological satellite services share the same frequency band. With the assumption that only the mean and the variance of the channel gains are available for the interference links, a framework for the network utility maximization subject to stochastic interference constraints, was formulated [25]. A survey was presented in [26] for database-assisted spectrum sharing in satellite communications, where a variety of historical and statistical CSI has been suggested to be stored and utilized for spectrum sharing. Energy efficient power allocation was investigated for cognitive satellite-terrestrial networks in [27]. The effective energy efficiency of the satellite links was maximized, while satisfying the statistical or instantaneous interference constraints imposed by the primary terrestrial links [27]. It has been demonstrated that large-scale-CSI-assisted spectrum sharing also has great potentials in improving the spectrum efficiency of hybrid networks [16], [25]–[27]. Similar to [20]–[23], opportunistic optimization across time was either not

considered or just considered for the terrestrial links in [16], [25]–[27]. The transmission characteristics for the involved satellite link/links were assumed to stay invariant within the considered time duration [16], [25]–[27].

To the best of our knowledge, no spectrum sharing scheme has been designed for hybrid satellite-UAV-terrestrial networks based on opportunistic transmission optimization across both frequency and time for all links in the satellite, UAV, and terrestrial components.

B. Main Contributions

Focusing on *fine-over-coarse* spectrum sharing based on large-scale CSI for a hybrid satellite-UAV-terrestrial MCN, the main contributions of our work are listed as follows.

- A framework is proposed for *fine-over-coarse* spectrum sharing in a hybrid satellite-UAV-terrestrial MCN, where the spectrum resource is utilized in terms of time-sliced subcarriers. In the framework, coordinated link scheduling is implemented based on subcarrier and time slice allocation for all links. To adapt to the Quality of Service (QoS) requirements of different vessel users, time slicing in the subcarriers is executed independently for V2S links and U2V and V2V links. Further, link-cluster-based scheduling with grouped time slice allocation is adopted for the V2S links. Accordingly, time-slice-oriented fine-grained spectrum sharing coordination can be carried out between V2S links and U2V and V2V links based on coarse time synchronization at time scales much larger than single time slices.
- An NP-hard mixed integer programming (MIP) problem is formulated for the coordinated scheduling of V2S, U2V, and V2V links in time-sliced subcarriers. In the problem formulation, a *worst-case* model is utilized to depict interference caused by V2S links as clusters. To solve the problem efficiently, the characteristics of its optimal solution is analyzed and a novel clustering algorithm is accordingly proposed for the delicate design of V2S link clusters. Along with V2S link clustering, a group of virtual cells, shaped by the distribution and QoS requirements of the vessel users, are formed within the large coverage area of the satellite, which largely facilitates spectrum sharing in the hybrid MCN.
- A suboptimal spectrum sharing scheme is proposed for the hybrid MCN, with the aid of the proposed link clustering algorithm and linear programming. Simulations results demonstrate that the proposed scheme has only a small performance gap as compared to benchmark, where the latter is obtained by optimal spectrum sharing with perfect fine-grained time synchronization over the time slices for all the links across the MCN.

II. System Model and Problem Formulation

A. System Model

Fig. 1 shows a hybrid satellite-UAV-terrestrial MCN. The satellite provides macro coverage for both service and signaling in the MCN. The UAVs and some of the vessels with

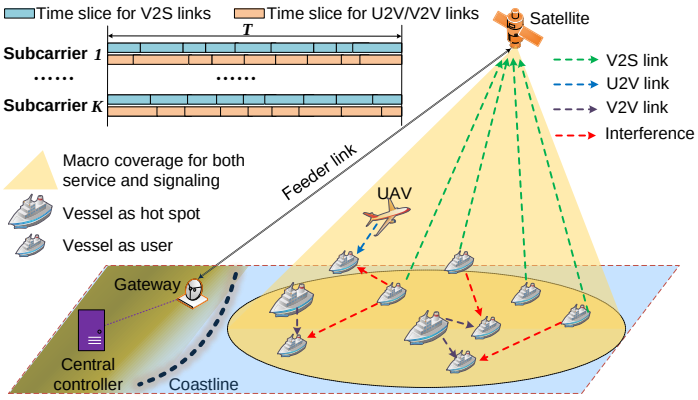

Fig. 1. Illustration of a hybrid satellite-UAV-terrestrial MCN.

spare communication capabilities provide hot-spot access for coverage enhancement. The vessels as users could be served either directly by the satellite or via the UAV/vessel-based hot spots. Assume that there are M UAVs and N vessels. Set $\mathbb{N}_1 = \{1, ..., N_1\}$, $\mathbb{N}_2 = \{N_1 + 1, ..., N_1 + N_2\}$, and $\mathbb{N}_3 = \{N_1 + N_2 + 1, ..., N_1 + N_2 + N_3\}$, with $N = N_1 + N_2 + N_3$. N_1 of the vessels, named $n_1 \in \mathbb{N}_1$, are served directly by the satellite in the uplink via V2S links, and N_2 of the vessels, named $n_2 \in \mathbb{N}_2$, are served by the UAVs and the other N_3 vessels, named $n_3 \in \mathbb{N}_3$, in the downlink via U2V and V2V links, with $N_2 \geq M + N_3$. The UAVs and the vessels $n_3 \in \mathbb{N}_3$ are assumed to be all equipped with antenna arrays, while each of the vessels $n_1 \in \mathbb{N}_1$ and $n_2 \in \mathbb{N}_2$ might be equipped with either a single antenna or an antenna array. For efficient spectrum utilization, the U2V and V2V links share the same frequency band with the V2S links, coordinated by a central controller. Global knowledge of the MCN that is needed for spectrum sharing, including CSI of the links and QoS requirements of the vessel users, could be obtained via the signaling channels provided by the satellite.

Suppose that K subcarriers are available for the MCN, each with a bandwidth of B. In the serving time with a duration of T, the V2S links serving the N_1 vessels $n_1 \in \mathbb{N}_1$ are scheduled in the subcarriers with time slicing, as illustrated in Fig. 1. Without loss of generality, we assume $N_1 \geq K$. The time slicing in each subcarrier could be even or uneven,[2] according to the QoS requirements of the vessels. To avoid collision, at most one V2S link is active in each subcarrier at each specific moment. At the same time, the U2V and V2V links for the N_2 vessels $n_2 \in \mathbb{N}_2$ share the K subcarriers with the V2S links opportunistically. Time slicing is also adopted for the scheduling of the U2V and V2V links in the subcarriers whenever necessary. To control interference, at most one U2V or V2V link is scheduled in each subcarrier at each specific moment. Besides, each of the vessels $n_1 \in \mathbb{N}_1$ and $n_2 \in \mathbb{N}_2$ can only be served in one subcarrier at each moment. To circumvent the challenge of fine-grained network-wide time synchronization, it is assumed that time-slice-oriented fine synchronization is only achieved locally and separately among

[2]In practical applications, time slots with the same duration can be utilized, and uneven time slicing could be achieved by uneven allocation of time slots.

the V2S links and among the U2V and V2V links. The scheduling of the V2S links and that of the U2V and V2V links are only coarsely synchronized at the time scale T. That is only coarse time synchronization at the time scale T, which could be much larger than the duration of a single time slice, is achieved across the MCN for spectrum sharing between the V2S links and the U2V and V2V links.

Due to the downward pointing of the antenna arrays on UAVs for the U2V links, as well as the down tilt of those on the vessels $n_3 \in \mathbb{N}_3$ for the V2V links, the interference from the U2V and V2V links to the V2S links is ignored [16]. Correspondingly, the received signal of the V2S and U2V/V2V links can be written as

$$y_{n_1}^{(s)} = R_{n_1}^{(s)} h_{n_1}^{(s,v)} T_{n_1}^{(v)} x_{n_1}^{(v)} + z^{(s)}, \tag{1a}$$

$$y_{n_2}^{(v)} = R_{n_2}^{(v)} h_{n_2}^{(v,uv)} T_{n_2}^{(uv)} x_{n_2}^{(uv)} + \hat{R}_{n_2,\hat{n}_{n_2}}^{(v)} \hat{h}_{n_2,\hat{n}_{n_2}}^{(v,v)} \hat{T}_{n_2,\hat{n}_{n_2}}^{(v)} x_{\hat{n}_{n_2}}^{(v)} + z^{(v)}. \tag{1b}$$

$y_{n_1}^{(s)}$ denotes the received signal at the satellite from vessel n_1, and $y_{n_2}^{(v)}$ is the received signal at vessel n_2 from the UAV or vessel that serves it. $|R_{n_1}^{(s)}|^2$, $h_{n_1}^{(s,v)}$, $|T_{n_1}^{(v)}|^2$, and $x_{n_1}^{(v)}$ are the receive antenna gain, the channel, the transmit antenna gain, and the transmit signal of the V2S link for vessel n_1, $|R_{n_2}^{(v)}|^2$, $h_{n_2}^{(v,uv)}$, $|T_{n_2}^{(uv)}|^2$, and $x_{n_2}^{(uv)}$ represent those of the U2V/V2V link for vessel n_2, and $|\hat{R}_{n_2,\hat{n}_{n_2}}^{(v)}|^2$, $\hat{h}_{n_2,\hat{n}_{n_2}}^{(v,v)}$, $|\hat{T}_{n_2,\hat{n}_{n_2}}^{(v)}|^2$, and $x_{\hat{n}_{n_2}}^{(v)}$ are those of the interference link from vessel $\hat{n}_{n_2}$ to n_2. $\hat{n}_{n_2} \in \mathbb{N}_1$ is the vessel served by the V2S link that interferes the U2V/V2V link serving vessel n_2. $z^{(s)}$ and $z^{(v)}$ denote the white Gaussian noise at the satellite and the vessels, respectively.

A composite channel model consisting of large-scale fading and small-scale fading is adopted for all the involved links [13], [14], [16], [29], [30]. Specifically, we have $h_{n_1}^{(s,v)} = \sqrt{l_{n_1}^{(s,v)}} w_{n_1}^{(s,v)}$, $h_{n_2}^{(v,uv)} = \sqrt{l_{n_2}^{(v,uv)}} w_{n_2}^{(v,uv)}$, and $\hat{h}_{n_2,\hat{n}_{n_2}}^{(v,v)} = \sqrt{\hat{l}_{n_2,\hat{n}_{n_2}}^{(v,v)}} \hat{w}_{n_2,\hat{n}_{n_2}}^{(v,v)}$, where $l_{n_1}^{(s,v)}$, $l_{n_2}^{(v,uv)}$, and $\hat{l}_{n_2,\hat{n}_{n_2}}^{(v,v)}$ denote the large-scale fading, $w_{n_1}^{(s,v)}$, $w_{n_2}^{(v,uv)}$, and $\hat{w}_{n_2,\hat{n}_{n_2}}^{(v,v)}$ are the small-scale fading, with $\mathbf{E}|w_{n_1}^{(s,v)}|^2 = 1$, $\mathbf{E}|w_{n_2}^{(v,uv)}|^2 = 1$, and $\mathbf{E}|\hat{w}_{n_2,\hat{n}_{n_2}}^{(v,v)}|^2 = 1$, and $\mathbf{E}$ is the expectation operator. The large-scale fading is mainly caused by the path loss, and the small-scale fading could be Rayleigh or Rician [28]. For the V2S links, the large-scale fading can be written as $l_{n_1}^{(s,v)}[\text{dB}] = \text{FSPL}(d_{n_1}^{(s,v)}, f_c) + \mathfrak{b}_{n_1}^{(s,v)}$ [29]–[31], where $\text{FSPL}(d_{n_1}^{(s,v)}, f_c)$ denotes the free space path loss, $d_{n_1}^{(s,v)}$ is the distance from vessel n_1 to the satellite, f_c is the center frequency of the subcarriers, and $\mathfrak{b}_{n_1}^{(s,v)}$ represents environment-related loss, such as the atmospheric attenuation [31]. When vessel n_2 is served via a U2V link, the large-scale fading $l_{n_2}^{(v,uv)}$ can be expressed as [32]

$$l_{n_2}^{(v,u)}[\text{dB}] = \frac{A}{1 + a e^{-b(\rho_{n_2}^{(v,u)} - a)}} + B_{n_2}^{(v,u)}, \tag{2}$$

where $A = \eta_{LOS} - \eta_{NLOS}$, $B_{n_2}^{(v,u)} = 20\log_{10}(d_{n_2}^{(v,u)}) + 20\log_{10}\left(\frac{4\pi f_c}{300}\right) + \eta_{NLOS}$, and $\rho_{n_2}^{(v,u)} = \frac{180}{\pi}\arcsin\left(\frac{\mathfrak{h}_{n_2}^{(u)}}{d_{n_2}^{(v,u)}}\right)$, with $d_{n_2}^{(v,u)}$ denoting the distance between vessel n_2 and the UAV that serves it, $\mathfrak{h}_{n_2}^{(u)}$ being the height of the UAV, f_c denoting the center frequency in MHz, and $\eta_{LOS}, \eta_{NLOS}, a, b$ representing environment-related constant parameters. Otherwise, if vessel n_2 is served via a V2V link, $l_{n_2}^{(v,uv)}$ can be expressed as [33]

$$l_{n_2}^{(v,v)}[\text{dB}] = C + (44.9 - 6.55\log_{10}\mathfrak{h}_{n_2}^{(vt)})\log_{10}\frac{d_{n_2}^{(v,v)}}{1000} + 45.5 + (35.46 - 1.1\mathfrak{h}_{n_2}^{(vr)})\log_{10} f_c - 13.82\log_{10}\mathfrak{h}_{n_2}^{(vr)} + 0.7\mathfrak{h}_{n_2}^{(vr)}, \tag{3}$$

where $d_{n_2}^{(v,v)}$ denotes the distance between vessel n_2 and vessel n_3 that serves it, $\mathfrak{h}_{n_2}^{(vt)}$ and $\mathfrak{h}_{n_2}^{(vr)}$ denote the antenna heights of vessel n_3 and n_2 respectively, and C is a constant parameter indicating the propagation environment. Similarly, the large-scale fading of the interference link from vessel n_1 to n_2 can be written as [33]

$$\hat{l}_{n_2,n_1}^{(v,v)}[\text{dB}] = C + (44.9 - 6.55\log_{10}\hat{\mathfrak{h}}_{n_1}^{(v)})\log_{10}\frac{d_{n_2,n_1}^{(v,v)}}{1000} + 45.5 + (35.46 - 1.1\hat{\mathfrak{h}}_{n_2}^{(v)})\log_{10} f_c - 13.82\log_{10}\hat{\mathfrak{h}}_{n_2}^{(v)} + 0.7\hat{\mathfrak{h}}_{n_2}^{(v)}, \tag{4}$$

in which $d_{n_2,n_1}^{(v,v)}$ is the distance between vessel n_1 and n_2, and $\hat{\mathfrak{h}}_{n_1}^{(v)}$ and $\hat{\mathfrak{h}}_{n_2}^{(v)}$ represent the antenna heights of vessel n_1 and n_2, respectively.

Compared to the fast-varying small-scale fading, the large-scale fading usually varies much more slowly. To be more friendly for practical applications, only large-scale CSI of the links, i.e., $l_{n_1}^{(s,v)}$, $l_{n_2}^{(v,uv)}$, and $\hat{l}_{n_2,n_1}^{(v,v)}$, $\forall n_1, n_2$, is utilized for spectrum sharing. Without loss of generality, we assume the large-scale CSI of each link is the same in different subcarriers. The acquisition of large-scale CSI could be accomplished via either centralized calculation based on the large-scale fading models, e.g., (2)-(4), or in a more precise way via distributed link-by-link estimation [34]–[36]. Due to the mobility of the UAVs, vessels, as well as the satellite, the transmission distances, i.e., $d_{n_1}^{(s,v)}$, $d_{n_2}^{(v,u)}$, $d_{n_2}^{(v,v)}$, and $d_{n_2,n_1}^{(v,v)}$, and correspondingly the large-scale CSI for the links, may vary slightly during the serving time T. Accordingly, average large-scale CSI could be utilized for spectrum sharing in T.

B. Problem Formulation

Because of the large coverage area of the satellite, different V2S links may cause distinctively different interference to the U2V and V2V links when they are scheduled in the same subcarriers simultaneously. To efficiently implement spectrum sharing with coarse time synchronization at the time scale T, we hope to delicately organize the V2S links into link clusters and adopt grouped time slice allocation for them in the K subcarriers in coordinated scheduling with the U2V and V2V links. Since the leaked interference from the U2V and V2V links to the V2S links is ignored, we consider the U2V and V2V links separately in terms of individual links for scheduling. To achieve a better energy efficiency while pursuing better spectrum utilization, the energy consumption of the MCN is minimized in spectrum sharing while guaranteeing the QoS for the vessels $n_1 \in \mathbb{N}_1$ and $n_2 \in \mathbb{N}_2$.

Let C_{V2S} denote the number of V2S link clusters. Note that $1 \leq C_{V2S} \leq N_1$, and it should be delicately designed based on the channel states of the links in the MCN. Set $\mathbb{K} = \{1, ..., K\}$ and $\mathbb{C} = \{1, ..., C_{V2S}\}$. Let $\delta_{n_1,c}$, $n_1 \in \mathbb{N}_1, c \in \mathbb{C}$, denote the cluster indicators for the V2S links. If the V2S link for vessel n_1 is in cluster c, we have $\delta_{n_1,c} = 1$, and otherwise $\delta_{n_1,c} = 0$. Further, let $\eta_{k,c}$ and θ_{k,n_2}, $k \in \mathbb{K}$, $c \in \mathbb{C}$, $n_2 \in \mathbb{N}_2$, represent the scheduling indicators for the V2S links clusters and the U2V/V2V links, respectively. If some link in the V2S link cluster c is scheduled in subcarrier k, then $\eta_{k,c} = 1$, and otherwise $\eta_{k,c} = 0$. Similarly, if the U2V/V2V link for vessel n_2 is scheduled in subcarrier k, then $\theta_{k,n_2} = 1$, and otherwise $\theta_{k,n_2} = 0$. It can be seen from (1) that when only the large-scale CSI is available, the transmission rates of the V2S and U2V/V2V links can be expressed as

$$\mathcal{R}_{n_1} = B\mathbf{E}_w \log_2(1 + \frac{|R_{n_1}^{(s)}|^2 l_{n_1}^{(s,v)} |w_{n_1}^{(s,v)}|^2 |T_{n_1}^{(v)}|^2 p_{n_1}^{(v)}}{{\sigma^{(s)}}^2}), \quad (5a)$$

$$\mathcal{R}_{n_2} = B\mathbf{E}_w \log_2(1 + \frac{|R_{n_2}^{(v)}|^2 l_{n_2}^{(v,uv)} |w_{n_2}^{(v,uv)}|^2 |T_{n_2}^{(uv)}|^2 p_{n_2}^{(uv)}}{\mathfrak{I}_{n_2} + {\sigma^{(v)}}^2}), \quad (5b)$$

in which $\mathbf{E}_w$ denotes the expectation operator with respect to the small-scale channel fading. $\mathfrak{I}_{n_2}$ is the interference suffered by the U2V/V2V link for vessel n_2, and

$$\begin{aligned} \mathfrak{I}_{n_2} &= \mathbf{E}_w \left[|\hat{R}_{n_2,\hat{n}_{n_2}}^{(v)}|^2 \hat{l}_{n_2,\hat{n}_{n_2}}^{(v,v)} |\hat{w}_{n_2,\hat{n}_{n_2}}^{(v,v)}|^2 |\hat{T}_{n_2,\hat{n}_{n_2}}^{(v)}|^2 p_{\hat{n}_{n_2}}^{(v)} \right] \\ &= |\hat{R}_{n_2,\hat{n}_{n_2}}^{(v)}|^2 \hat{l}_{n_2,\hat{n}_{n_2}}^{(v,v)} |\hat{T}_{n_2,\hat{n}_{n_2}}^{(v)}|^2 p_{\hat{n}_{n_2}}^{(v)}. \end{aligned} \quad (6)$$

$p_{n_1}^{(v)} = \mathbf{E}|x_{n_1}^{(v)}|^2$, $p_{n_2}^{(uv)} = \mathbf{E}|x_{n_2}^{(uv)}|^2$, and $p_{\hat{n}_{n_2}}^{(v)} = \mathbf{E}|x_{\hat{n}_{n_2}}^{(v)}|^2$ are the transmit power of the corresponding links. With coarse time synchronization at the time scale equal to the serving time T, when the U2V/V2V link for the vessel n_2 is scheduled in subcarrier k, i.e., $\theta_{k,n_2} = 1$, it can be determined that

$$\hat{n}_{n_2} \in \mathfrak{N}_k = \{n_1 | \eta_{k,c} = 1, \delta_{n_1,c} = 1, c \in \mathbb{C}, n_1 \in \mathbb{N}_1\}. \quad (7)$$

Note that $\mathfrak{N}_k$ is empty if subcarrier k is not allocated to any V2S link cluster, i.e., $\eta_{k,c} = 0$ for all c. Correspondingly, when the U2V/V2V link for the vessel n_2 is scheduled in subcarrier k, we introduce a *worst-case* model to depict the interference and replace $\mathfrak{I}_{n_2}$ by its upper bounds $\bar{\mathfrak{I}}_{n_2,k}$ in the spectrum sharing optimization, with

$$\bar{\mathfrak{I}}_{n_2,k} = \begin{cases} \max\limits_{n_1 \in \mathfrak{N}_k} |\hat{R}_{n_2,n_1}^{(v)}|^2 \hat{l}_{n_2,n_1}^{(v,v)} |\hat{T}_{n_2,n_1}^{(v)}|^2 p_{n_1}^{(v)}, & \mathfrak{N}_k \neq \phi, \\ 0, & \mathfrak{N}_k = \phi. \end{cases} \quad (8)$$

Further, $\mathcal{R}_{n_2}$ given by (5b) is replaced by its lower bound as

$$\underline{\mathcal{R}}_{n_2,k} = B\mathbf{E}_w \log_2(1 + \frac{|R_{n_2}^{(v)}|^2 l_{n_2}^{(v,uv)} |w_{n_2}^{(v,uv)}|^2 |T_{n_2}^{(uv)}|^2 p_{n_2}^{(uv)}}{\bar{\mathfrak{I}}_{n_2,k} + {\sigma^{(v)}}^2}). \quad (9)$$

To guarantee the QoS for the vessels $n_1 \in \mathbb{N}_1$ and $n_2 \in \mathbb{N}_2$, we assume that a minimum data volume $V_n^{QoS} > 0$, $n \in \mathbb{N}_1 \cup \mathbb{N}_2$, is required to be transmitted for vessel n within a time duration of T. With a serving time of $\tau_{n,k}$ for vessel $n \in \mathbb{N}_1 \cup \mathbb{N}_2$ in subcarrier k, the total energy consumption of the MCN for transmission can be written as

$$E_{total} = \sum_{n_1=1}^{N_1} p_{n_1}^{(v)} \sum_{k=1}^{K} \tau_{n_1,k} + \sum_{n_2=N_1+1}^{N_1+N_2} p_{n_2}^{(uv)} \sum_{k=1}^{K} \tau_{n_2,k}. \quad (10)$$

With the target of minimizing E_{total} while guaranteeing the QoS for the vessels, the spectrum sharing problem is formulated as

$$\min_{\{C_{V2S}, \delta_{n_1,c}, \eta_{k,c}, \theta_{k,n_2}, \tau_{n_1,k}, \tau_{n_2,k}\}} E_{total} \quad (11a)$$

$$s.t. \ \mathcal{R}_{n_1} \sum_{k \in \mathfrak{k}_{n_1}} \tau_{n_1,k} \geq V_{n_1}^{QoS}, n_1 \in \mathbb{N}_1, \quad (11b)$$

$$\sum_{k=1}^{K} \theta_{k,n_2} \underline{\mathcal{R}}_{n_2,k} \tau_{n_2,k} \geq V_{n_2}^{QoS}, n_2 \in \mathbb{N}_2, \quad (11c)$$

$$\sum_{k=1}^{K} \tau_{n_1,k} \leq T, \ \sum_{k=1}^{K} \tau_{n_2,k} \leq T, \forall n_1, n_2, \quad (11d)$$

$$\sum_{n_1=1}^{N_1} \tau_{n_1,k} \leq T, \sum_{n_2=N_1+1}^{N_1+N_2} \tau_{n_2,k} \leq T, \forall k, \quad (11e)$$

$$1 \leq C_{V2S} \leq N_1, \tau_{n_1,k} \geq 0, \ \tau_{n_2,k} \geq 0, \forall k, n_1, n_2, \quad (11f)$$

$$\delta_{n_1,c} \in \{0,1\}, \eta_{k,c} \in \{0,1\}, \theta_{k,n_2} \in \{0,1\}, \forall n_1, n_2, k, c, \quad (11g)$$

where

$$\mathfrak{k}_{n_1} = \{k | \delta_{n_1,c} = 1, \eta_{k,c} = 1, c \in \mathbb{C}, k \in \mathbb{K}\}. \quad (12)$$

(11b) and (11c) are for the QoS guarantees for the vessels $n_1 \in \mathbb{N}_1$ and $n_2 \in \mathbb{N}_2$, (11d) is to assure that each of the vessels can only be served in one subcarrier at each moment, and (11e) indicates that at most one V2S link and one U2V/V2V link are active in each subcarrier. Note that $\underline{\mathcal{R}}_{n_2,k}$ is a function of $\delta_{n_1,c}$ and $\eta_{k,c}$, as shown in (7)–(9).

It is worth noting that in order to reserve as much flexibility as possible, the mapping between the V2S links and the V2S link clusters is not restricted in the problem formulation in (11), and neither is that between the subcarriers and the V2S link clusters. A single V2S link is allowed to belong to different V2S link clusters simultaneously, and a subcarrier may also be allocated to more than one V2S link clusters.

III. Proposed Spectrum Sharing Scheme with Shaped Virtual Cells

A. Analysis on the Spectrum Sharing Problem

It can be seen from (11) and (7)-(9) that the link-cluster-based spectrum sharing problem is a complicated NP-hard MIP problem, and it is rather challenging to find an optimal solution for it directly [37], [38]. Thus, before solving the problem, we firstly uncover some characteristics of its optimal solution.

Suppose that

$$\begin{aligned} \mathbb{S} = \{ & C_{V2S}, \delta_{n_1,c}, \eta_{k,c}, \theta_{k,n_2}, \tau_{n_1,k}, \tau_{n_2,k} \\ & | \, c \in \mathbb{C}, n_1 \in \mathbb{N}_1, n_2 \in \mathbb{N}_2, k \in \mathbb{K}\}, \end{aligned} \quad (13)$$

is a solution for (11) with a total energy consumption of E_{total} given by (10). If there exist any $\bar{k} \in \mathbb{K}$, $\bar{k}' \in \mathbb{K}$ and $\bar{c} \in \mathbb{C}$

that satisfy $\bar{k} \neq \bar{k}'$ and $\eta_{\bar{k},\bar{c}}\eta_{\bar{k}',\bar{c}} = 1$, it can be known from the following Lemma 1 that we can find a new solution $\mathbb{S}'$ for (11) that is better than, or at least equally good as $\mathbb{S}$, by separating the V2S links scheduled in the subcarriers $\bar{k}$ and $\bar{k}'$ and splitting the V2S link cluster $\bar{c}$ into two.

Lemma 1: For any solution $\mathbb{S}$ of (11), as given in (13), with a total energy consumption of E_{total}, if there exist any $\bar{k} \in \mathbb{K}$, $\bar{k}' \in \mathbb{K}$ and $\bar{c} \in \mathbb{C}$ that satisfy $\bar{k} \neq \bar{k}'$ and $\eta_{\bar{k},\bar{c}}\eta_{\bar{k}',\bar{c}} = 1$, then a new solution $\mathbb{S}' = \{C'_{V2S}, \delta'_{n_1,c}, \eta'_{k,c}, \theta'_{k,n_2}, \tau'_{n_1,k}, \tau'_{n_2,k} \,|\, c \in \mathbb{C}', n_1 \in \mathbb{N}_1, n_2 \in \mathbb{N}_2, k \in \mathbb{K}\}$ could be found for (11), in which $C'_{V2S} = C_{V2S} + 1$, $\mathbb{C}' = \{1, ..., C'_{V2S}\}$, and

$$\eta'_{k,c} = \begin{cases} 1, & k = \bar{k}', c = C'_{V2S}, \\ 0, & k \in \mathbb{K} \setminus \{\bar{k}'\}, c = C'_{V2S}, \\ 0, & k = \bar{k}', c = \bar{c}, \\ \eta_{k,c}, & \text{otherwise}. \end{cases} \tag{14}$$

Besides, $E'_{total} \leq E_{total}$ holds with $E'_{total} = \sum_{n_1=1}^{N_1} p_{n_1}^{(v)} \sum_{k=1}^{K} \tau'_{n_1,k} + \sum_{n_2=N_1+1}^{N_1+N_2} p_{n_2}^{(uv)} \sum_{k=1}^{K} \tau'_{n_2,k}$.

Proof 1: See Appendix A.

Alternatively, suppose that for $\mathbb{S}$ given in (13), there are a group of $\bar{c}_1$, $\bar{c}_2$ and $\bar{k}$ satisfying $\eta_{\bar{k},\bar{c}_1}\eta_{\bar{k},\bar{c}_2} = 1$, and $\eta_{k,\bar{c}_1} = 0$, $\eta_{k,\bar{c}_2} = 0$ for all $k \in \mathbb{K} \setminus \{\bar{k}\}$. Without loss of generality, it is assumed that $\bar{c}_1 = C_{V2S} - 1$ and $\bar{c}_2 = C_{V2S}$.[3] By merging the V2S link cluster $\bar{c}_1$ and $\bar{c}_2$ in $\mathbb{S}$ into one, we can get

$$\begin{aligned} \mathbb{S}'' = \{&C''_{V2S}, \delta''_{n_1,c}, \eta''_{k,c}, \theta''_{k,n_2}, \tau''_{n_1,k}, \tau''_{n_2,k} \\ &| \, c \in \mathbb{C}'', n_1 \in \mathbb{N}_1, n_2 \in \mathbb{N}_2, k \in \mathbb{K}\}, \end{aligned} \tag{15}$$

where $C''_{V2S} = C_{V2S} - 1$, $\mathbb{C}'' = \{1, ..., C''_{V2S}\}$,

$$\delta''_{n_1,c} = \begin{cases} \delta_{n_1,C_{V2S}-1} + \delta_{n_1,C_{V2S}}, & n_1 \in \mathbb{N}_1, c = C''_{V2S}, \\ \delta_{n_1,c}, & \text{otherwise}, \end{cases} \tag{16}$$

$\eta''_{k,c} = \eta_{k,c}$ for all $k \in \mathbb{K}$ and $c \in \mathbb{C}''$, and $\theta''_{k,n_2} = \theta_{k,n_2}$, $\tau''_{n_1,k} = \tau_{n_1,k}$, $\tau''_{n_2,k} = \tau_{n_2,k}$ for all $k \in \mathbb{K}$, $n_1 \in \mathbb{N}_1$ and $n_2 \in \mathbb{N}_2$. It can be inferred from the problem formulation in (11) that $\mathbb{S}''$ is a feasible solution equally good as $\mathbb{S}$.

Based on the $\mathbb{S}''$ given in (15) and the $\mathbb{S}'$ sketched in Lemma 1, the following Theorem 1 can be derived. It gives us some clues for solving the problem (11) in the selection of the number of V2S link clusters, as well as the mapping between the subcarriers and the V2S link clusters. Specially, Theorem 1 reveals that if (11) is a feasible problem, an optimal solution could always be found by allocating one subcarrier to each V2S link cluster exclusively. It is worth noting that the mapping between the V2S links and the V2S link clusters is not restricted in Theorem 1. In other words, a particular V2S link is allowed to belong to different V2S link clusters simultaneously, as mentioned in the end of Section II.

Theorem 1: When the spectrum sharing problem in (11) is feasible, and $\lceil (\sum_{n_1=1}^{N_1} V_{n_1}^{QoS}/R_{n_1})/T \rceil = K'$, there must be an optimal solution $\mathbb{S}^*$ for (11) with $K' \leq C^*_{V2S} \leq K$, $\sum_{k=1}^{K} \eta^*_{k,c} = 1$ for all $c \in \mathbb{C}^*$ with $\mathbb{C}^* = \{1, ..., C^*_{V2S}\}$, and $\sum_{c=1}^{C^*_{V2S}} \eta^*_{k,c} \leq 1$ for all $k \in \mathbb{K}$. If $K' = K$, then there is an optimal solution $\mathbb{S}^*$ with $C^*_{V2S} = K$, $\sum_{k=1}^{K} \eta^*_{k,c} = 1$ for all $c \in \mathbb{C}^*$, and $\sum_{c=1}^{C^*_{V2S}} \eta^*_{k,c} = 1$ for all $k \in \mathbb{K}$.

Proof 2: See Appendix B.

Further, for any feasible group of C_{V2S}, $\delta_{n_1,c}$, $\eta_{k,c}$, $n_1 \in \mathbb{N}_1$, $k \in \mathbb{K}, c \in \mathbb{C}$, the scheduling of the U2V and V2V links in the K subcarriers, i.e., θ_{k,n_2}, $k \in \mathbb{K}$, $n_2 \in \mathbb{N}_2$, as well as the serving time for all the vessels, i.e., $\tau_{n_1,k}$, $\tau_{n_2,k}$, $n_1 \in \mathbb{N}_1$, $n_2 \in \mathbb{N}_2$, $k \in \mathbb{K}$, can be optimally determined via linear programming [39], as illustrated in Theorem 2.

Theorem 2: For any fixed $C_{V2S}, \delta_{n_1,c}, \eta_{k,c}$, $n_1 \in \mathbb{N}_1$, $k \in \mathbb{K}, c \in \mathbb{C}$, if the problem in (11) is feasible, then the optimal $\tau_{n_1,k}$, $n_1 \in \mathbb{N}_1$, $k \in \mathbb{K}$, can be obtained by finding a feasible point for the following group of linear constraints

$$\mathcal{R}_{n_1} \sum_{k \in \mathbb{k}_{n_1}} \tau_{n_1,k} = V_{n_1}^{QoS}, n_1 \in \mathbb{N}_1, \tag{17a}$$

$$\sum_{k \in \mathbb{k}_{n_1}} \tau_{n_1,k} \leq T, \sum_{n_1=1}^{N_1} \tau_{n_1,k} \leq T, n_1 \in \mathbb{N}_1, k \in \mathbb{k}_{n_1}, \tag{17b}$$

$$\tau_{n_1,k} \geq 0, n_1 \in \mathbb{N}_1, k \in \mathbb{k}_{n_1}, \tag{17c}$$

$$\tau_{n_1,k} = 0, n_1 \in \mathbb{N}_1, k \notin \mathbb{k}_{n_1}, \tag{17d}$$

and the optimal θ_{k,n_2} and $\tau_{n_2,k}$ can be derived based on the linear programming problem

$$\min_{\{\tau_{n_2,k}\}} \sum_{n_2=N_1+1}^{N_1+N_2} p_{n_2}^{(uv)} \sum_{k=1}^{K} \tau_{n_2,k} \tag{18a}$$

$$s.t. \sum_{k=1}^{K} \mathcal{R}_{n_2,k} \tau_{n_2,k} \geq V_{n_2}^{QoS}, n_2 \in \mathbb{N}_2, \tag{18b}$$

$$\sum_{k=1}^{K} \tau_{n_2,k} \leq T, \sum_{n_2=N_1+1}^{N_1+N_2} \tau_{n_2,k} \leq T, n_2 \in \mathbb{N}_2, k \in \mathbb{K}, \tag{18c}$$

$$\tau_{n_2,k} \geq 0, \forall n_2, k, \tag{18d}$$

and the equations

$$\theta_{k,n_2} = \begin{cases} 1, & \tau_{n_2,k} > 0, \\ 0, & \tau_{n_2,k} = 0, \end{cases} \quad \forall k, n_2. \tag{19}$$

Proof 3: See Appendix C.

B. Link Clustering with Shaped Virtual Cells

It can be inferred from Theorem 1 that in an optimal solution for the spectrum sharing problem in (11), the V2S links scheduled in the same subcarrier could be taken as a link cluster. Furthermore, Theorem 2 indicates that once the V2S link clusters are formed and fit into the subcarriers appropriately, i.e., $C_{V2S}, \delta_{n_1,c}, \eta_{k,c}$, $n_1 \in \mathbb{N}_1$, $k \in \mathbb{K}, c \in \mathbb{C}$, are appropriately determined, the problem (11) can be solved with linear programming immediately. With these inspirations, we detail the clustering of the V2S links in this subsection.

Intuitively, with the worst-case interference model adopted in (11), the V2S links that may cause similar interference to the U2V and V2V links should be grouped together, so that the diversity of the V2S links in inter-link interference could be reserved and opportunistically utilized for spectrum sharing.

[3] It can always be achieved by changing the order of the V2S link clusters in $\mathbb{S}$.

Suppose that the MCN is in a full-load state with respect to the available subcarriers, i.e., $(\sum_{n_1=1}^{N_1} V_{n_1}^{QoS}/R_{n_1})/T = K$.[4] It can be known from Theorem 1 that an optimal spectrum sharing scheme could be derived by grouping the V2S links into K clusters, with each cluster occupying one of the K subcarriers exclusively. Besides, it is noted that the impact of inter-link interference is closely coupled with the geographical distribution, as well as QoS requirements, of the vessels n_1 and n_2. Thus, clustering of the V2S links can be seen as forming K *virtual cells* for the vessels n_1 in the large coverage area of the satellite, *shaped* by the distribution and QoS requirements of all vessel users. Each *shaped virtual cell* is allocated one subcarrier exclusively, and the U2V and V2V links for the vessels n_2 share the subcarriers opportunistically, based on the profile of the interference caused to the V2S links in each virtual cell.

To carry out V2S link clustering, we define a feature vector for each of the V2S links to depict their similarity in the interference caused to the U2V and V2V links, as

$$\mathcal{F}_{n_1} = \left[\frac{V_{N_1+1}^{QoS}}{\hat{\mathcal{R}}_{N_1+1}^{(n_1)}} p_{n_2}^{(uv)}, ..., \frac{V_{N_1+N_2}^{QoS}}{\hat{\mathcal{R}}_{N_1+N_2}^{(n_1)}} p_{n_2}^{(uv)} \right], \tag{20}$$

where

$$\hat{\mathcal{R}}_{n_2}^{(n_1)} = B\mathbf{E}_w \log_2(1+\frac{|R_{n_2}^{(v)}|^2 l_{n_2}^{(v,uv)} |w_{n_2}^{(v,uv)}|^2 |T_{n_2}^{(uv)}|^2 p_{n_2}^{(uv)}}{\hat{\mathfrak{I}}_{n_2}^{(n_1)} + {\sigma^{(v)}}^2}), \tag{21}$$

is the transmission rate of the U2V/V2V link for vessel n_2 when it is scheduled in the same subcarrier with the V2S link for vessel n_1, and $\hat{\mathfrak{I}}_{n_2}^{(n_1)} = |\hat{R}_{n_2,n_1}^{(v)}|^2 \hat{l}_{n_2,n_1}^{(v,v)} |\hat{T}_{n_2,n_1}^{(v)}|^2 p_{n_1}^{(v)}$. Further, the similarity between the V2S link for vessel $n_1 \in \mathbb{N}_1$ and that for $n_1' \in \mathbb{N}_1$ is measured by the distance between their feature vectors, which is defined based on L1 norm as [40]

$$\mathcal{D}_{n_1,n_1'} = ||\mathcal{F}_{n_1} - \mathcal{F}_{n_1'}||_1 = \sum_{n_2 \in \mathbb{N}_2} \left| \frac{V_{n_2}^{QoS}}{\hat{\mathcal{R}}_{n_2}^{(n_1)}} - \frac{V_{n_2}^{QoS}}{\hat{\mathcal{R}}_{n_2}^{(n_1')}} \right| p_{n_2}^{(uv)}. \tag{22}$$

Note that $\mathcal{F}_{n_1}$ and $\mathcal{D}_{n_1,n_1'}$ are defined based on the target utility of (11), i.e., the energy consumption of the MCN. With $\mathcal{F}_{n_1}$ and $\mathcal{D}_{n_1,n_1'}$, we propose a V2S link clustering algorithm based on a modified K-means method [41], as illustrated in Algorithm 1.

The fundamental idea of Algorithm 1 is grouping the V2S links with close distance between their feature vectors into one cluster. Specially, the QoS requirement of the V2S links shown in (11b) is also considered in the clustering. The main steps of Algorithm 1 are further explained as follows.

1) Set the number of the V2S clusters, i.e., C_{V2S}, as K, and select K feature vectors of the V2S links as the initial centers of the clusters.
2) Calculate the distance between the feature vectors of all the V2S links and the centers of the K V2S link clusters, and following the *smallest-distance-first* principle, group each V2S link into the cluster[5] that is *unsaturated for the QoS guarantees* and has the center that is closest to the feature vector of the V2S link.
3) Update the center of each V2S link cluster, by setting it as average of the feature vectors of the V2S links belonging to the cluster, and repeat 2)-3) until convergence.

The *smallest-distance-first* principle assures that the V2S links with a smaller distance to the cluster centers are always grouped first. Besides, a cluster is judged as being *unsaturated for the QoS guarantees* when the subcarrier k allocated to it is not fully occupied in the time duration of T, i.e.,

$$\sum_{n_1=1}^{N_1} \tau_{n_1,k} < T. \tag{23}$$

Note that the V2S link for the vessel n_1 will remain waiting to be clustered, i.e., $n_1 \in \bar{\Phi}$, even if it has already been clustered into some of the K clusters, until the required time for the transmission of its minimum data volume $V_{n_1}^{QoS}$, i.e., $V_{n_1}^{QoS}/\mathcal{R}_{n_1}$, is satisfied. Furthermore, the allocated time for the V2S links in the K subcarriers, i.e., $\tau_{n_1,k}$, $n_1 \in \mathbb{N}_1$, $k \in \mathbb{K}$, are also obtained at the end of Algorithm 1.

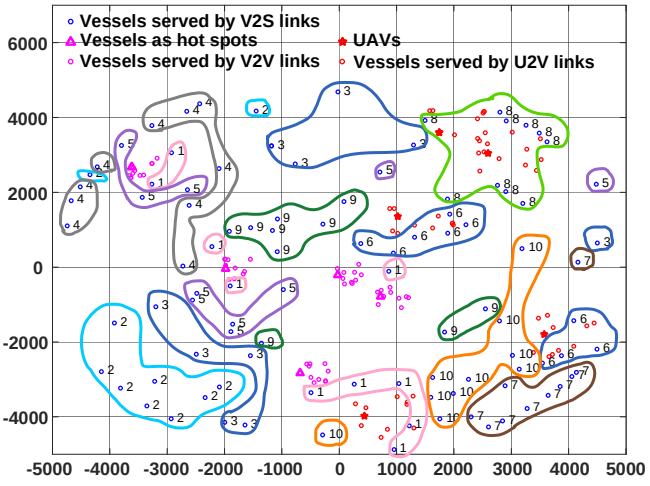

Fig. 2. Shaped virtual cells formed via V2S link clustering in Algorithm 1.

Fig. 2 shows the shaped virtual cells formed by the V2S link clustering algorithm. It is obtained based on a random topology of the MCN considered in the simulations later in Section IV, within a circular area of a radius of 5000m. The shaped virtual cells corresponding to different V2S link clusters are indicated by closed lines with different colors. The vessels $n_1 \in \mathbb{N}_1$ circled by the line/lines with the same color belong to the same virtual cell. The number next to each of the vessel $n_1 \in \mathbb{N}_1$ served by the V2S links indicates the index of the shaped virtual cell it belongs to. It can be observed that the shaped virtual cells formed for spectrum sharing could be rather diversified in shapes, with an ability to adapt to both the geographical distribution and the QoS requirements of the links in the MCN. Further, based on the convergence of the

[4]It is consistent with the background that spectrum sharing between the serving links for the vessels $n_1 \in \mathbb{N}_1$ and $n_2 \in \mathbb{N}_2$ is necessary, so as to guarantee the QoS for the vessels within the available spectrum resource.

[5]Note that one V2S link may belong to multiple clusters simultaneously, to assure that the required minimum data volume $V_{n_1}^{QoS}$ could be transmitted within the time duration of T.

Algorithm 1 Proposed V2S link clustering algorithm

Set $C_{V2S}=K$, and allocate subcarrier k to the V2S link cluster $c=k$, $k=1,...,K$.
Select K feature vectors of the V2S links, i.e., $\mathcal{F}_{\acute{n}_i}$, $i=1...,K$, $\acute{n}_i \in \mathbb{N}_1$, as the initial centers for the V2S link clusters, i.e., $\mathfrak{c}_j$, $j=1,...,K$.
Let $\Phi_c, c=1,...,C_{V2S}$, represent the set of the V2S links in the C_{V2S} clusters, respectively.
Set $\delta=10^{-2}$, $\mathcal{D}_0^{sum}=0$, $\mathcal{D}_1^{sum}=\sum_{n_1=1}^{N_1}||\mathcal{F}_{n_1}||_1$.
while $|\mathcal{D}_0^{sum}-\mathcal{D}_1^{sum}|/\mathcal{D}_1^{sum}>\delta$ **do**
  Set $\mathcal{D}_0^{sum}=\mathcal{D}_1^{sum}$ and $\mathcal{D}_1^{sum}=0$.
  for $n_1=1,...,N_1$ **do**
    for $j=1,...,K$ **do**
      Calculate the distance between the V2S link for vessel n_1 and the center of the jth cluster based on (22), and denote it as $\hat{\mathcal{D}}_{n_1,j}=||\mathcal{F}_{n_1}-\mathfrak{c}_j||_1$.
    end for
  end for
  Let $\bar{\Phi}$ denote the set of the V2S links that wait to be clustered, and initialize $\bar{\Phi}=\{1,...,N_1\}$ and $\Phi_j=\phi, j=1,...,K$.
  Initialize the serving time for all the vessels n_1 in the K subcarriers as $\tau_{n_1,k}=0$, $n_1\in\mathbb{N}_1$, $k\in\mathbb{K}$.
  while $\bar{\Phi}\neq\phi$ **do**
    Find $\{n_1^*,j^*\}=\arg\min_{n_1,j}\hat{\mathcal{D}}_{n_1,j}$, and calculate the unoccupied time in the subcarrier allocated to the V2S cluster j^*, i.e., $\Delta t_{j^*}=T-\sum_{n_1=1}^{N_1}\tau_{n_1,j^*}$, to judge whether it is *unsaturated for the QoS guarantees*.
    if $\Delta t_{j^*}>0$ **then**
      Cluster the V2S link for vessel n_1^* into cluster j^*, and set $\Phi_{j^*}:=\Phi_{j^*}\cup\{n_1^*\}$, $\hat{\mathcal{D}}_{n_1^*,j^*}=+\infty$, and $\mathcal{D}_1^{sum}:=\mathcal{D}_1^{sum}+||\mathcal{F}_{n_1^*}-\mathfrak{c}_{j^*}||_1$.
      Calculate the serving time that could be allocated to the V2S link for vessel n_1^* in cluster j^*, i.e., $\tau_{n_1^*,j^*}:=\min\{V_{n_1^*}^{QoS}/\mathcal{R}_{n_1^*}-\sum_{k=1}^{K}\tau_{n_1^*,k},\Delta t_{j^*}\}$.
      if $\sum_{k=1}^{K}\tau_{n_1^*,k}=V_{n_1^*}^{QoS}/\mathcal{R}_{n_1^*}$ **then**
        Set $\bar{\Phi}:=\bar{\Phi}\setminus\{n_1^*\}$.
      end if
    end if
  end while
  Update the centers for the K V2S link clusters as $\mathfrak{c}_j=\frac{1}{|\Phi_j|}\sum_{n_1\in\Phi_j}\mathcal{F}_{n_1}$, $j=1,...,K$.
end while

K-means method [41], it can be inferred that Algorithm 1 is assured to converge. Actually, simulations show that it can converge with less than 10 iterations for the MCN considered in Section IV.

C. Proposed Spectrum Sharing Scheme

Based on the characteristics of the optimal solution for the problem (11) uncovered in Subsection III-A, and the V2S link clustering algorithm proposed in Subsection III-B, we proceed to propose a suboptimal spectrum sharing scheme for the hybrid MCN in Algorithm 2.

The fundamental idea of Algorithm 2 is firstly clustering the V2S links into K clusters and scheduling them in the K subcarriers, respectively, and then scheduling the U2V and V2V links in the subcarriers opportunistically. Specifically, the proposed scheme consists of three parts: 1) selection of the initial centers for K V2S link clusters, 2) clustering of the V2S links into K clusters based on Algorithm 1, and 3) scheduling of the U2V and V2V links in the K subcarriers based on Theorem 2. By Algorithm 2, a solution could be derived for the spectrum sharing problem in (11) as

$$\begin{aligned}\hat{\mathbb{S}}=&\{\hat{C}_{V2S},\hat{\delta}_{n_1,c},\hat{\eta}_{k,c},\hat{\theta}_{k,n_2},\hat{\tau}_{n_1,k},\hat{\tau}_{n_2,k}\\&|\,c\in\hat{\mathbb{C}},n_1\in\mathbb{N}_1,n_2\in\mathbb{N}_2,k\in\mathbb{K}\}.\end{aligned}\tag{24}$$

with $\hat{\mathbb{C}}=\{1,...,\hat{C}_{V2S}\}$ and $\hat{C}_{V2S}=K$. Specially, as illustrated in Step 3 of Algorithm 2, when K V2S link clusters $\Phi_c, c\in\hat{\mathbb{C}}$, and $\hat{\tau}_{n_1,k}$, $n_1\in\mathbb{N}_1$, $k\in\mathbb{K}$, have been obtained based on Algorithm 1, $\hat{\delta}_{n_1,c}$ and $\hat{\eta}_{k,c}$, $n_1\in\mathbb{N}_1$, $c\in\hat{\mathbb{C}}$, $k\in\mathbb{K}$, can be respectively written as

$$\hat{\delta}_{n_1,c}=\begin{cases}1,\ n_1\in\Phi_c,\\0,\ n_1\notin\Phi_c,\end{cases}\tag{25}$$

$$\hat{\eta}_{k,c}=\begin{cases}1,\ k=c,\\0,\ k\neq c.\end{cases}\tag{26}$$

Further, to solve the linear programming problem (18) as illustrated in Step 4, $\underline{\mathcal{R}}_{n_2,k}$ in (18b) should be firstly calculated based on (7)-(9) and $\hat{C}_{V2S}$, $\hat{\delta}_{n_1,c}$, and $\hat{\eta}_{k,c}$, $n_1\in\mathbb{N}_1$, $c\in\hat{\mathbb{C}}$, $k\in\mathbb{K}$, obtained in Step 3. Here, $\mathfrak{N}_k$ given in (7) could accordingly be rewritten as

$$\mathfrak{N}_k=\Phi_k, k=1,...,K.\tag{27}$$

For efficient calculation of $\mathcal{R}_{n_1}$ and $\underline{\mathcal{R}}_{n_2,k}$ given by (5a) and (9) during the execution of Algorithm 2, closed-form expressions are introduced for them based on approximations. By assuming that the small scale fading of the V2S and the U2V links follows the Rician distribution and that of the V2V links follows the Rayleigh distribution, $\mathcal{R}_{n_1}$ and $\underline{\mathcal{R}}_{n_2,k}$ can be respectively rewritten as [14], [42]

$$\mathcal{R}_{n_1}=\log_2(e)e^{\frac{1+\kappa_1}{\bar{\chi}_{n_1}^{(s,v)}}}\sum_{i=0}^{\infty}E_{i+1}\left(\frac{1+\kappa_1}{\bar{\chi}_{n_1}^{(s,v)}}\right)\mathcal{P}(i,\kappa_1),\tag{28}$$

$$\underline{\mathcal{R}}_{n_2,k}=\begin{cases}\underline{\mathcal{R}}_{n_2,k}^{(v,u)},\ \text{if vessel } n_2 \text{ is served by a U2V link},\\\underline{\mathcal{R}}_{n_2,k}^{(v,v)},\ \text{if vessel } n_2 \text{ is served by a V2V link},\end{cases}\tag{29}$$

where

$$\underline{\mathcal{R}}_{n_2,k}^{(v,u)}=\log_2(e)e^{\frac{1+\kappa_2}{\bar{\chi}_{n_2,k}^{(v,u)}}}\sum_{i=0}^{\infty}E_{i+1}\left(\frac{1+\kappa_2}{\bar{\chi}_{n_2,k}^{(v,u)}}\right)\mathcal{P}(i,\kappa_2),\tag{30a}$$

$$\begin{aligned}\underline{\mathcal{R}}_{n_2,k}^{(v,v)}=&\log_2\left(1+\frac{|R_{n_2}^{(v)}|^2 l_{n_2}^{(v,v)}|T_{n_2}^{(uv)}|^2 p_{n_2}^{(uv)}}{\lambda_{n_2,k}(\bar{\mathfrak{I}}_{n_2,k}+{\sigma^{(v)}}^2)}\right)\\&+\log_2(\lambda_{n_2,k})-\log_2(e)(1-\lambda_{n_2,k}^{-1}).\end{aligned}\tag{30b}$$

$E_{i+1}(.)$ is the exponential integral, and $\mathcal{P}(i,\kappa_1)=\gamma(i,\kappa_1)/\Gamma(i)$, $\mathcal{P}(i,\kappa_2)=\gamma(i,\kappa_2)/\Gamma(i)$ are regularized

Algorithm 2 Proposed spectrum sharing scheme for the MCN

1: Let $\hat{\mathbb{S}} = \{\hat{C}_{V2S}, \hat{\delta}_{n_1,c}, \hat{\eta}_{k,c}, \hat{\theta}_{k,n_2}, \hat{\tau}_{n_1,k}, \hat{\tau}_{n_2,k} \,|\, c \in \hat{\mathbb{C}}, n_1 \in \mathbb{N}_1, n_2 \in \mathbb{N}_2, k \in \mathbb{K}\}$ denote a solution for the spectrum sharing problem in (11).
2: Select the initial centers for the K V2S link clusters, i.e., $\mathcal{F}_{\acute{n}_i}$, $i = 1..., K$, $\acute{n}_i \in \mathbb{N}_1$, via Algorithm 3.
3: Cluster the V2S links into K clusters based on Algorithm 1, and get $\hat{C}_{V2S} = K$, the V2S link clusters $\Phi_c, c \in \hat{\mathbb{C}}$, and $\hat{\tau}_{n_1,k} = \tau_{n_1,k}$, $n_1 \in \mathbb{N}_1$, $k \in \mathbb{K}$. Then derive $\hat{\delta}_{n_1,c}$ and $\hat{\eta}_{k,c}$, $n_1 \in \mathbb{N}_1$, $c \in \hat{\mathbb{C}}$, $k \in \mathbb{K}$, based on (25) and (26) respectively.
4: Schedule the U2V and V2V links in the K subcarriers based on Theorem 2, and get $\hat{\tau}_{n_2,k}$ and $\hat{\theta}_{k,n_2}$, $n_2 \in \mathbb{N}_2$, $k \in \mathbb{K}$, based on the solving of the linear programming problem in (18) and the equations in (19).

gamma functions, $\bar{\chi}_{n_1}^{(s,v)} = \frac{|R_{n_1}^{(s)}|^2 l_{n_1}^{(s,v)} |T_{n_1}^{(v)}|^2 p_{n_1}^{(v)}}{\sigma^{(s)^2}}$, and $\lambda_{n_2,k} = 1 + \frac{|R_{n_2}^{(v)}|^2 l_{n_2}^{(v,v)} |T_{n_2}^{(uv)}|^2 p_{n_2}^{(uv)}}{(\bar{\gamma}_{n_2,k} + \sigma^{(v)^2}) + \lambda_{n_2,k}^{-1} |R_{n_2}^{(v)}|^2 l_{n_2}^{(v,v)} |T_{n_2}^{(uv)}|^2 p_{n_2}^{(uv)}}$. Similarly, $\hat{\mathcal{R}}_{n_2}^{(n_1)}$ in the feature vectors for the V2S links, as given in (21), can be efficiently calculated in the same way as $\underline{\mathcal{R}}_{n_2,k}$.

In Algorithm 2, the selection of the initial centers for the K V2S link clusters in Step 2, i.e., $\mathcal{F}_{\acute{n}_i}$, $i = 1..., K$, $\acute{n}_i \in \mathbb{N}_1$, is also critical for the performance of the proposed spectrum sharing scheme. As illustrated in Algorithm 3, a greedy method is adopted to find the first K feature vectors of the V2S links with the largest distance to each other to act as the initial centers for the K V2S link clusters. To ensure that there is a large distance between any two of the K feature vectors selected by Algorithm 3, a *compound* distance is introduced to measure the distance from one V2S link to multiple other V2S links. Specially, the *compound* distance from the V2S link for vessel n_1 to those for the vessels $\tilde{n}_1, ..., \tilde{n}_{i-1}$ is expressed as

$$D_{n_1,\tilde{n}_1,...,\tilde{n}_{i-1}}^{\text{CMPD}} = \prod_{j=1}^{i-1} \mathcal{D}_{n_1,\tilde{n}_j}. \tag{31}$$

Simulations in Section IV demonstrate that the proposed link-cluster-based *fine-over-coarse* spectrum sharing scheme can achieve a significant performance gain in both energy efficiency and spectrum efficiency for the hybrid satellite-UAV-terrestrial MCN. Furthermore, it is shown that the proposed scheme has only a small performance gap to the benchmark set by optimal spectrum sharing based on perfect network-wide fine-grained time synchronization. With both low complexity and high flexibility for implementation, the proposed spectrum sharing scheme is quite promising for practical applications.

Algorithm 3 Initial center selection for K V2S link clusters

1: **for** $n_1 = 1, ..., N_1$ **do**
2: **for** $n_1' = 1, ..., n_1 - 1, n_1 + 1, ..., N_1$ **do**
3: Calculate the distance between the V2S link for vessel n_1 and that for vessel n_1' i.e., $\mathcal{D}_{n_1,n_1'}$, based on (22).
4: **end for**
5: **end for**
6: Find $\{\tilde{n}_1, \tilde{n}_2\} = \arg\max_{n_1,n_1'} \mathcal{D}_{n_1,n_1'}$, and set the feature vectors $\mathcal{F}_{\tilde{n}_1}$ and $\mathcal{F}_{\tilde{n}_2}$ as the initial centers for the first two V2S link clusters, i.e., $\acute{n}_1 = \tilde{n}_1$, $\acute{n}_2 = \tilde{n}_2$, and $\mathcal{F}_{\acute{n}_1} = \mathcal{F}_{\tilde{n}_1}$, $\mathcal{F}_{\acute{n}_2} = \mathcal{F}_{\tilde{n}_2}$.
7: **for** $i = 3, ..., K$ **do**
8: Find the V2S link with the largest *compound* distance to the V2S links for the vessels $\tilde{n}_1, ..., \tilde{n}_{i-1}$ based on (31), i.e., $\tilde{n}_i = \arg\max_{n_1} \prod_{j=1}^{i-1} \mathcal{D}_{n_1,\tilde{n}_j}$.
9: Set the feature vector $\mathcal{F}_{\tilde{n}_i}$ as the initial center for the ith V2S link cluster, i.e., $\acute{n}_i = \tilde{n}_i$ and $\mathcal{F}_{\acute{n}_i} = \mathcal{F}_{\tilde{n}_i}$.
10: **end for**

IV. Simulations and Discussions

In the simulations, we consider a hybrid satellite-UAV-terrestrial MCN with $M = 5$, $N = 205$, $N_1 = 100$, $N_2 = 100$, $N_3 = 5$, $K = 10$, $f_c = 2$GHz, and $B = 1$MHz. Suppose that the satellite is deployed in an orbit with an altitude of 1000km, and the UAVs are deployed at the height of 200m, i.e., $\mathfrak{h}_{n_2}^{(u)} = 200$m for all $n_2 \in \mathbb{N}_2$. The UAVs and the vessels are all assumed to be randomly distributed in a circular area $\mathcal{A}$ with a radius of 5km within the coverage area of the satellite. Each UAV serves 10 of the vessels $n_2 \in \mathbb{N}_2$ located in the circular area of a radius of 1000m around it, and each vessel $n_3 \in \mathbb{N}_3$ serves 10 of the vessels $n_2 \in \mathbb{N}_2$ located in the circular area of a radius of 500m around it. The serving time duration is set as $T = 10$s, during which the sub-satellite point is assumed to be located at $\mathcal{L}_s = (115°E, 10°N)$ or $(125°E, 10°N)$, and the center of $\mathcal{A}$ is at $(110°E, 10°N)$.

All the vessels $n_1 \in \mathbb{N}_1$ are supposed to be equipped with an antenna array with an aperture of 0.5m, the pattern of which follows the recommendation ITU-R S.465, as shown in Fig. 3 [43]. Correspondingly, the transmit antenna gain of the vessels $n_1 \in \mathbb{N}_1$ for the V2S links is $|T_{n_1}^{(v)}|^2 = 18.5$dBi, and that for the interference link to each vessel n_2, i.e., $|\hat{T}_{n_2,\hat{n}_{n_2}}^{(v)}|^2$, is dependent on the off-axis angle. Each vessel $n_2 \in \mathbb{N}_2$ is assumed to be equipped with a single omni antenna, and thus $|R_{n_2}^{(v)}|^2$ and $|\hat{R}_{n_2,\hat{n}_{n_2}}^{(v)}|^2$ are all 0dBi. The receive antenna gain of the satellite $|R_{n_1}^{(s)}|^2$ for the V2S links is supposed to be 25dBi, and the transmit antenna gain of the UAVs for the U2V links and that of the vessels $n_3 \in \mathbb{N}_3$ for the V2V links, i.e., $|T_{n_2}^{(uv)}|^2$, are set as 5dBi. The transmit power of the vessels $n_1 \in \mathbb{N}_1$ for the V2S links is set as $p_{n_1}^{(v)} = 30$dBm, and that of the UAVs and the vessels $n_3 \in \mathbb{N}_3$ for the U2V and V2V links are set as $p_{n_2}^{(uv)} \in [0, 20]$dBm. The noise power is set as $\sigma^{(s)^2} = \sigma^{(v)^2} = -114$dBm. The channel parameters for the V2S and U2V links are set as $\mathfrak{b}_{n_1}^{(s,v)} = 1$dB, $a = 5.0188$, $b = 0.3511$, $\eta_{LOS} = 2.3$, and $\eta_{NLOS} = 34$ [32]. The antenna height of the vessels $n_1 \in \mathbb{N}_1$ and $n_2 \in \mathbb{N}_2$ is assumed to be 10m, and that of the vessels $n_3 \in \mathbb{N}_3$ is 30m, i.e., $\mathfrak{h}_{n_2}^{(vt)} = 30$m, $\mathfrak{h}_{n_2}^{(vr)} = 10$m, $\hat{\mathfrak{h}}_{n_1}^{(v)} = 10$m, and $\hat{\mathfrak{h}}_{n_2}^{(v)} = 10$m. The small-scale fading for the V2V links is assumed to follow the Rayleigh distribution, and that for the V2S and the U2V links is assumed to be Rician distributed, the K-factors of which are respectively set as 0.3 and 0.5.

Without loss of generality, the QoS of the vessels is set

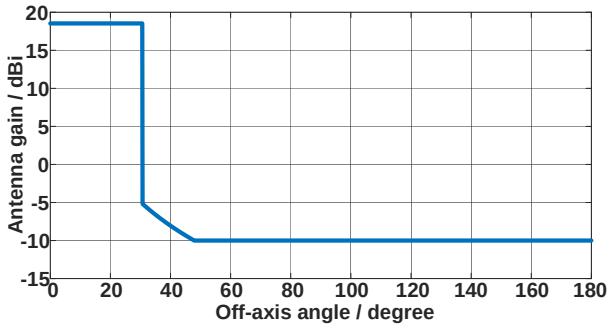

Fig. 3. Antenna pattern for the vessels $n_1 \in \mathbb{N}_1$ following ITU-R S.465.

in proportion to the transmission rates of the V2S, U2V and V2V links, i.e., $V_{n_1}^{QoS} = (KT/N_1)\mathcal{R}_{n_1}$ and $V_{n_2}^{QoS} = \min_{n_1} \hat{\mathcal{R}}_{n_2}^{(n_1)} + \alpha(\max_{n_1} \hat{\mathcal{R}}_{n_2}^{(n_1)} - \min_{n_1} \hat{\mathcal{R}}_{n_2}^{(n_1)})$, $n_1 \in \mathbb{N}_1$, $n_2 \in \mathbb{N}_2$. Note that larger α indicates more stringent QoS for the vessels n_2, and the problem (11) may be infeasible when $\alpha \in [0, 1)$ is too large for some MCN topologies. In the simulations, only feasible MCN topologies are considered for the selected α.

A. Performance of the Proposed Spectrum Sharing Scheme

Note that with the above setting of $V_{n_1}^{QoS}$, the K subcarriers will be fully occupied by the V2S links for QoS guarantees, i.e., $\sum_{n_1=1}^{N_1}\sum_{k=1}^{K}\tau_{n_1,k} = \sum_{n_1=1}^{N_1} KT/N_1 = KT$. Further, with fixed $p_{n_1}^{(v)}$, the energy consumption of the V2S links, i.e., $\sum_{n_1=1}^{N_1} p_{n_1}^{(v)}\sum_{k=1}^{K}\tau_{n_1,k} = \sum_{n_1=1}^{N_1} p_{n_1}^{(v)} KT/N_1$, is a constant irrelevant to the link scheduling. Thus, only the energy consumption of the U2V and V2V links, i.e., $\hat{E}_{total} = \sum_{n_2=N_1+1}^{N_1+N_2} p_{n_2}^{(uv)}\sum_{k=1}^{K}\tau_{n_2,k}$, is considered and demonstrated in the following.

The energy consumption with the proposed spectrum sharing scheme in the serving time $T = 10$s for $\alpha = 0, 1/2, 2/3$, $\mathcal{L}_s = (125°E, 10°N)$ and $\alpha = 2/3$, $\mathcal{L}_s = (115°E, 10°N)$ is shown in Figs. 4–7. The energy consumption in Figs. 4–7 is obtained by averaging over 10 random topologies of the MCN, and thus a total of 40 topologies are considered. For comparison, the performance of three benchmark schemes are also shown, which are denoted as the optimal scheme, Random-I scheme, and Random-II scheme, respectively. The optimal scheme is derived based on optimal spectrum sharing among individual V2S, U2V and V2S links with perfect fine-grained network-wide time synchronization. The Random-I scheme is obtained based on random clustering of the V2S links and optimal scheduling of the U2V and V2V links via Theorem 2. The Random-II scheme is a completely random scheme with both random clustering, of the V2S links, and random scheduling, of the U2V and V2V links. The number of V2S link clusters is also set as K in the Random-I and Random-II scheme.

The optimal scheme actually acts as a lower-bound benchmark for the proposed scheme in energy consumption, and is expressed as

$$\hat{\mathbb{S}} = \{\hat{C}_{V2S}^*, \hat{\delta}_{n_1,c}^*, \hat{\tau}_{n_1}^*, \hat{\tau}_{n_2,n_1}^* | c \in \hat{\mathbb{C}}^*, n_1 \in \mathbb{N}_1, n_2 \in \mathbb{N}_2\}, \tag{32}$$

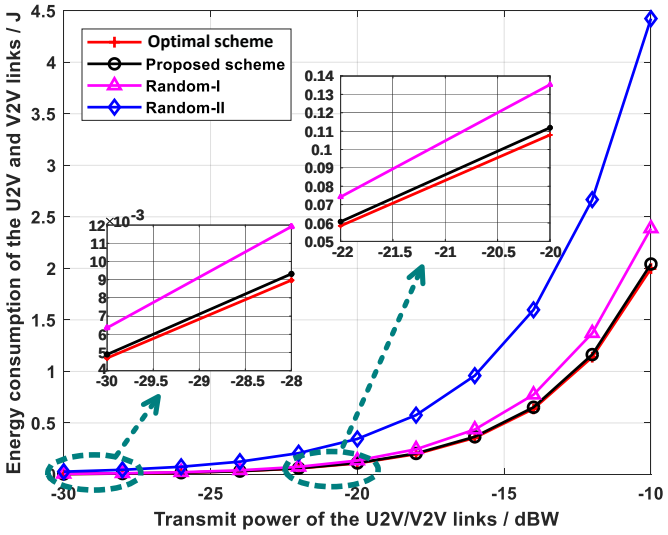

Fig. 4. Energy consumption for $\alpha = 0$, $\mathcal{L}_s = (125°E, 10°N)$.

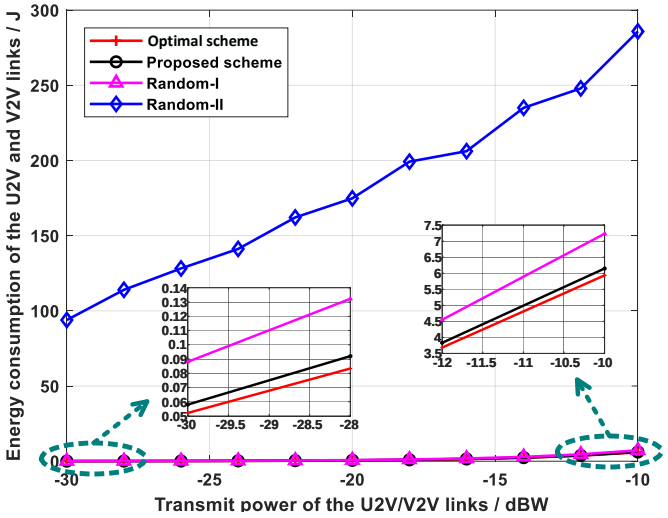

Fig. 5. Energy consumption for $\alpha = 1/2$, $\mathcal{L}_s = (125°E, 10°N)$.

where $\hat{C}_{V2S}^* = N_1$, $\hat{\mathbb{C}}^* = \{1, ..., \hat{C}_{V2S}^*\}$, $\hat{\delta}_{n_1,c}^* = 1$ for $n_1 = c$ and $\hat{\delta}_{n_1,c}^* = 0$ for $n_1 \neq c$, $\hat{\tau}_{n_1}^* = KT/N_1$, and $\hat{\tau}_{n_2,n_1}^*$, $n_2 \in \mathbb{N}_2$, $n_1 \in \mathbb{N}_1$, are obtained by solving

$$\min_{\{\tau_{n_2,n_1}\}} \sum_{n_2=N_1+1}^{N_1+N_2} p_{n_2}^{(uv)} \sum_{k=1}^{K} \tau_{n_2,n_1} \tag{33a}$$

$$s.t. \sum_{n_1=1}^{N_1} \hat{\mathcal{R}}_{n_2}^{(n_1)} \tau_{n_2,n_1} \geq V_{n_2}^{QoS}, \forall n_2, \tag{33b}$$

$$\sum_{n_1=1}^{N_1} \tau_{n_2,n_1} \leq T, \sum_{n_2=N_1+1}^{N_1+N_2} \tau_{n_2,n_1} \leq \hat{\tau}_{n_1}^*, \forall n_2, n_1, \tag{33c}$$

$$\tau_{n_2,n_1} \geq 0, \forall n_2, n_1. \tag{33d}$$

Compared to the problem formulation in (11), the V2S links are considered individually in scheduling in (33). In the Random-I scheme, with random clustering of the V2S links, the QoS is guaranteed by cooperatively optimizing the scheduling of random V2S clusters and the U2V and the V2V

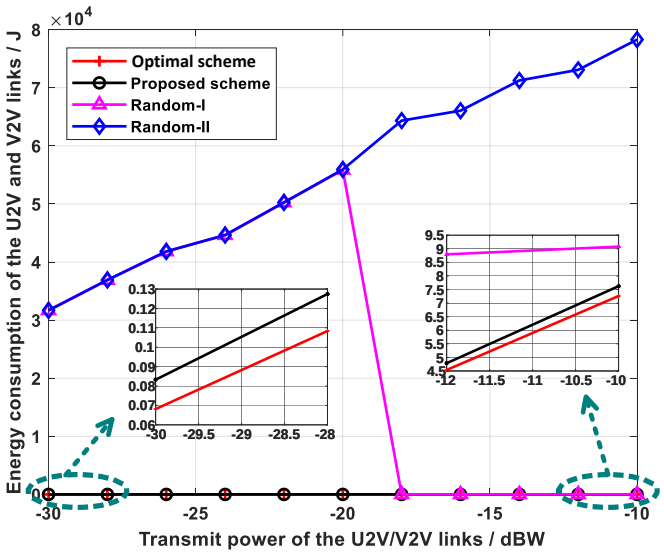

Fig. 6. Energy consumption for $\alpha = 2/3$, $\mathcal{L}_s = (125°E, 10°N)$.

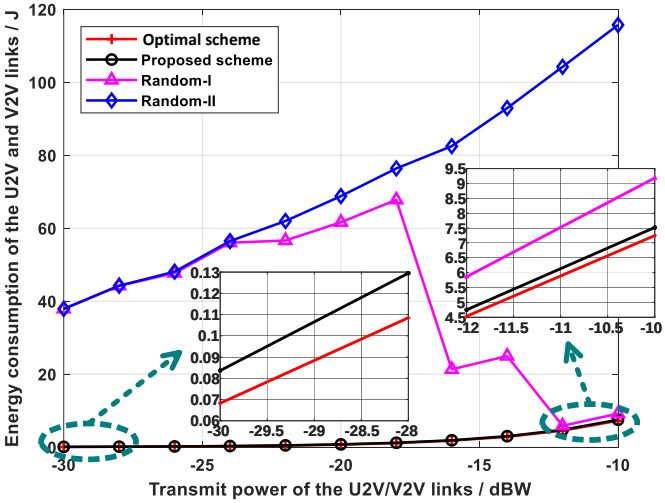

Fig. 7. Energy consumption for $\alpha = 2/3$, $\mathcal{L}_s = (115°E, 10°N)$.

links in the subcarriers. In the Random-II scheme, with both random link clustering and scheduling, the QoS is assured by adjusting the serving time for the U2V and V2V links, and when $T = 10$s is not enough, the serving time is extended until the required $V_{n_2}^{QoS}$ is transmitted. Further, when the link scheduling based on random link clustering is not feasible for the QoS guarantees in the Random-I scheme, the result achieved by the Random-II scheme is adopted instead.

It is shown by Figs. 4–7 that the proposed scheme achieves a significant performance gain in reducing the energy consumption compared to the Random-I and Random-II scheme. Furthermore, the proposed scheme has only a small performance gap from the lower bound achieved by the optimal spectrum sharing with the assumption of perfect fine-grained network-wide time synchronization. Note that the sudden turning point/points on the curve of the Random-I scheme in Fig. 6 and Fig. 7 is/are due to the variation of the feasibility of the scheme in ensuring the QoS for the U2V/V2V links along with the SNR. In some of the 10 topologies, the Random-I

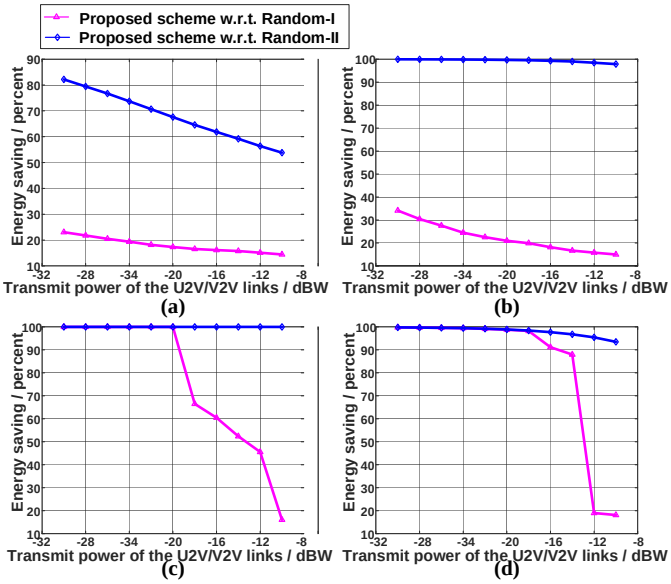

Fig. 8. Energy saving by the proposed spectrum sharing scheme, with (a)–(d) corresponding to Figs. 4–7 respectively.

scheme is infeasible in the lower SNR region and feasible in the higher SNR region. The performance gain of the proposed scheme with respect to (w.r.t) the Random-I and Random-II scheme in energy saving is presented in Fig. 8, with (a)–(d) corresponding to Figs. 4–7 respectively. It can be seen that compared to the Random-I scheme, the energy consumption of the U2V and V2V links could be saved for more than 20% in the low SNR region and more than 15% in the high SNR region. The percentage of energy saving goes up to more than 50% compared to the Random-II scheme. Since the transmission rate of the U2V/V2V links given in (9) is more sensitive to interference at low transmit power, a larger performance gain is observed in the low SNR region. Specially, Figs. 5–7 and Fig. 8(b)–(d) show that the proposed scheme saves more than 90% of the energy compared to the Random-II scheme. The reason is that severe inter-link interference tends to happen with both random V2S link clustering and U2V/V2V link scheduling. Accordingly, much more energy is needed to guarantee the QoS requirements of the vessel users for the Random-II scheme. Besides, Figs. 4–6 and Fig. 8(a)–(c) show that for larger α, i.e., for a group of larger $V_{n_2}^{QoS}$, more transmission energy is needed, and the proposed scheme promises a larger performance gain compared to the Random-I and Random-II schemes.

Note that the elevation angle at the center of the area $\mathcal{A}$ with respect to the satellite is $21°$ for $\mathcal{L}_s = (125°E, 10°N)$, and it is $56°$ for $\mathcal{L}_s = (115°E, 10°N)$. It can be inferred from Fig. 3 that when $\mathcal{L}_s = (125°E, 10°N)$, some of the vessels $n_2 \in \mathbb{N}_2$ may be within the main lobe of the antenna arrays of the vessels $n_1 \in \mathbb{N}_1$, while for $\mathcal{L}_s = (115°E, 10°N)$, all the vessels $n_2 \in \mathbb{N}_2$ will be out of the main lobe of the antenna arrays. Thus, the interference from the V2S links to the U2V and the V2V links tends to be more severe for $\mathcal{L}_s = (125°E, 10°N)$ than that for $\mathcal{L}_s = (115°E, 10°N)$. It can be observed that a large difference in energy consumption exists

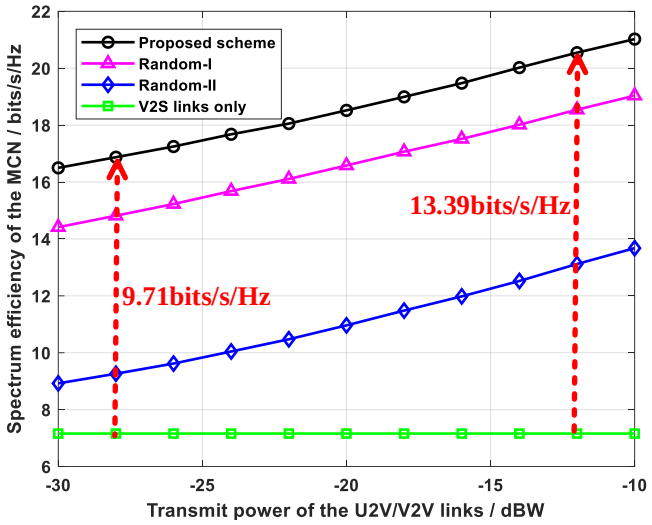

Fig. 9. Spectrum Efficiency for $\alpha = 0$, $\mathcal{L}_s = (125°E, 10°N)$.

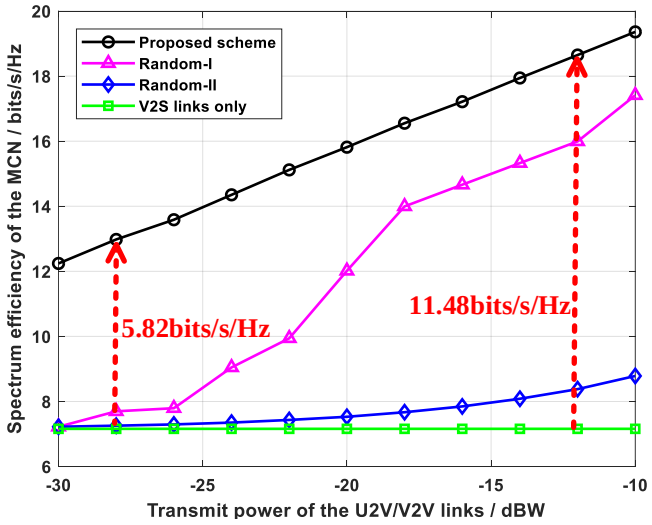

Fig. 10. Spectrum Efficiency for $\alpha = 2/3$, $\mathcal{L}_s = (125°E, 10°N)$.

between Fig. 6 and Fig. 7 for the Random-I and Random-II scheme. Contrarily, the proposed scheme performs well in both cases, keeping a small performance gap to the optimal scheme.

B. Improvement in Spectrum Efficiency for the MCN

The spectrum efficiency[6] achieved by the proposed scheme, the Random-I scheme, and the Random-II scheme for $\alpha = 0, 2/3$, $\mathcal{L}_s = (125°E, 10°N)$ and $\alpha = 2/3$, $\mathcal{L}_s = (115°E, 10°N)$ is shown in Figs. 9–11. The spectrum efficiency with only the V2S links is also presented for comparison.

In Figs. 9–11, a prominent improvement in the spectrum efficiency is observed with the proposed scheme. Besides, compared to the Random-I and Random-II scheme, the proposed scheme achieves a much more superior performance.

[6]The spectrum efficiency is calculated based on the data volume V_n^{QoS}, $n = n_1$ or n_2, and the practically-occupied spectrum bandwidth by the links.

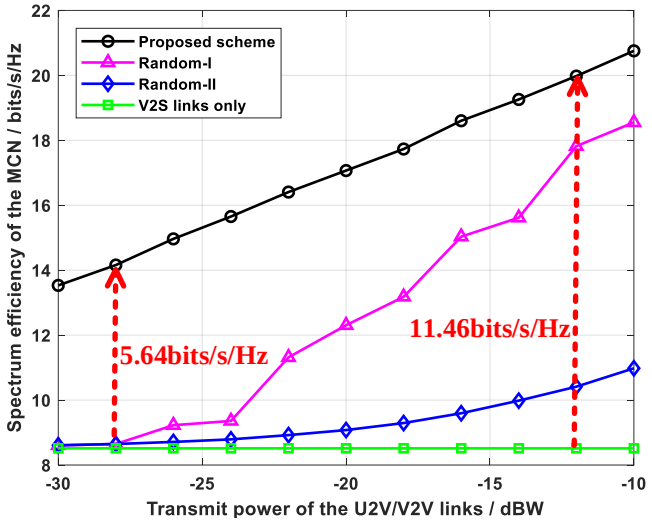

Fig. 11. Spectrum Efficiency for $\alpha = 2/3$, $\mathcal{L}_s = (115°E, 10°N)$.

Further, a decrease of the spectrum efficiency achieved by the proposed scheme is observed from Fig. 9 to Fig. 10. It is due to the fact that the spectrum efficiency is derived based on the QoS requirements of the vessels. In the simulations, a group of smaller $V_{n_2}^{QoS}$ is required for smaller α. Thus, there are more opportunities for the scheduling optimization of the U2V and the V2V links when α is smaller, and a larger performance gain could be obtained correspondingly.

What's more, Fig. 10 and Fig. 11 show that nearly the same spectrum efficiency improvement is achieved with the proposed scheme for $\alpha = 2/3$, $\mathcal{L}_s = (125°E, 10°N)$ and $\alpha = 2/3$, $\mathcal{L}_s = (115°E, 10°N)$, compared to the case with only the V2S links. As illustrated above, with smaller elevation angles of the V2S links, the interference from the V2S links to the U2V and the V2V links for $\mathcal{L}_s = (125°E, 10°N)$ tends to be more severe, compared to that for $\mathcal{L}_s = (115°E, 10°N)$. It indicates that the proposed scheme is effective in interference control for spectrum sharing in the hybrid MCN.

V. Conclusions

A fine-over-coarse spectrum sharing framework has been investigated for a hybrid satellite-UAV-terrestrial MCN based on large-scale CSI. With the target of minimizing the energy consumption, an NP-hard MIP problem is formulated. Based on the characteristics of the optimal solution for the problem, a novel V2S link clustering algorithm has been proposed, and a group of shaped virtual cells are formed within the large coverage area of the hybrid MCN. A suboptimal spectrum sharing scheme is then proposed, by which time-slice-oriented spectrum sharing can be carried out with coarse time synchronization at time scales much larger than single time slices. Simulations demonstrate that the proposed scheme can achieve a significant performance gain in terms of both energy efficiency and spectrum efficiency for the MCN. With the advantages of both low complexity and high flexibility, the proposed scheme is quite promising for practical applications.

APPENDIX A
PROOF OF LEMMA 1

Based on $\eta'_{k,c}$ given in (14), a group of clustering indicators for the V2S links in $\mathbb{S}'$, i.e., $\delta'_{n_1,c}$, $n_1 \in \mathbb{N}_1$, $c \in \mathbb{C}'$, could be obtained from those in $\mathbb{S}$ by splitting the C_{VS}-th cluster in $\mathbb{S}$ into two new ones, i.e., Cluster C_{VS} and $C'_{V2S} = C_{V2S} + 1$, while keeping the others unchanged. By defining $\mathbb{N}_1^{(sub)} = \{n_1 | \delta_{n_1,\bar{c}} = 1, \tau_{n_1,\bar{k}'} > 0, n_1 \in \mathbb{N}_1\}$, $\delta'_{n_1,c}$ can be set as

$$\delta'_{n_1,c} = \begin{cases} 1, & n_1 \in \mathbb{N}_1^{(sub)}, c = C'_{V2S}, \\ 0, & n_1 \in \mathbb{N}_1 \setminus \mathbb{N}_1^{(sub)}, c = C'_{V2S}, \\ \delta_{n_1,c}, & \text{otherwise.} \end{cases} \tag{34}$$

Set $\mathfrak{N}'_k = \{n_1 | \eta'_{k,c} = 1, \delta'_{n_1,c} = 1, c = 1, ..., C'_{V2S}, n_1 = 1, ..., N_1\}$, $k \in \mathbb{K}$, based on (7). Then we have $\mathfrak{N}'_k \subseteq \mathfrak{N}_k$, $k \in \mathbb{K}$. Further, a group of $\underline{\mathcal{R}}'_{n_2,k}$ could be derived based on $\mathfrak{N}'_k$ and (8), (9). Calculate $\underline{\mathcal{R}}_{n_2,k}$ based on (7)–(9) and the $\eta_{k,c}$, $\delta_{n_1,c}$ in $\mathbb{S}$, and it can be inferred that $\underline{\mathcal{R}}'_{n_2,k} \geq \underline{\mathcal{R}}_{n_2,k}$, $k \in \mathbb{K}$.

Let $\theta'_{k,n_2} = \theta_{k,n_2}$, $\tau'_{n_1,k} = \tau_{n_1,k}$, and

$$\tau'_{n_2,k} = \frac{\underline{\mathcal{R}}_{n_2,k} \tau_{n_2,k}}{\underline{\mathcal{R}}'_{n_2,k}}. \tag{35}$$

Then we have $\tau'_{n_2,k} \leq \tau_{n_2,k}$ for all $n_2 \in \mathbb{N}_2$, $k \in \mathbb{K}$. As $\mathbb{S}$ is a solution to the problem in (11), it can be derived that $\mathbb{S}'$ satisfies all the constraints in (11b)-(11g), and $E'_{total} \leq E_{total}$.

APPENDIX B
PROOF OF THEOREM 1

Suppose that $\mathbb{S}$ given by (13) is an optimal solution to (11), and there is one $\hat{k} \in \mathbb{K}$ that doesn't satisfy $\sum_{c=1}^{C_{V2S}} \eta_{\hat{k},c} \leq 1$, i.e., $\sum_{c=1}^{C_{V2S}} \eta_{\hat{k},c} > 1$. Assume that $\sum_{c=1}^{C_{V2S}} \eta_{\hat{k},c} = Z$ with $Z > 1$, and $\eta_{\hat{k},\hat{c}_z} = 1$, $z = 1, ..., Z$, where $\hat{c}_z \in \mathbb{C}$ and $\hat{c}_1 \neq \hat{c}_2 \neq ... \neq \hat{c}_Z$. It can be known that for all $z = 1, ..., Z$, either $\sum_{k=1}^{K} \eta_{k,\hat{c}_z} > 1$ or $\sum_{k=1}^{K} \eta_{k,\hat{c}_z} = 1$ holds. For any $\hat{c}_z$ satisfying $\sum_{k=1}^{K} \eta_{k,\hat{c}_z} = \Omega_z$ with $\Omega_z > 1$, it can be inferred from Lemma 1 that a solution with $C_{VS} + \Omega_z - 1$ V2S link clusters can be derived from $\mathbb{S}$. By applying Lemma 1 on $\mathbb{S}$ with respect to all $\hat{c}_z$ satisfying $\sum_{k=1}^{K} \eta_{k,\hat{c}_z} > 1$ successively, a solution $\mathbb{S}'$ with $C'_{VS} = C_{VS} + \sum_{z=1}^{Z} (\Omega_z - 1)$ and $\sum_{k=1}^{K} \eta'_{k,c} = 1$ for all $c \in \mathbb{C}'$ could be finally obtained for (11).

In the obtained solution $\mathbb{S}'$, we have $\sum_{c=1}^{C'_{VS}} \sum_{k=1}^{K} \eta'_{k,c} \leq C'_{VS}$. When $\lceil (\sum_{n_1=1}^{N_1} V_{n_1}^{QoS} / R_{n_1}) / T \rceil = K'$, i.e., at least K' subcarriers are needed for the QoS guarantees of the V2S links, $C'_{VS} \geq K'$ must hold; otherwise $\mathbb{S}'$ can't be a feasible solution for (11). Further, set $\mathbb{S} = \mathbb{S}'$, and for any $\hat{k}' \in \mathbb{K}$ that satisfies $\sum_{c=1}^{C'_{V2S}} \eta'_{\hat{k}',c} \geq 1$, merge the V2S link clusters c with $\eta'_{\hat{k}',c} = 1$ into one based on (15) and (16). After merging the V2S link clusters for all $\hat{k}' \in \mathbb{K}$ satisfying $\sum_{c=1}^{C'_{V2S}} \eta'_{\hat{k}',c} \geq 1$, a solution $\mathbb{S}''$ as shown in (15) can be obtained for (11). It can be inferred from Lemma 1 and the illustrations on (15) and (16) that $\mathbb{S}''$ is an optimal solution for (11) with $K' \leq C''_{VS} \leq K$, $\sum_{k=1}^{K} \eta''_{k,c} = 1$, $c \in \mathbb{C}''$, and $\sum_{c=1}^{C''_{VS}} \eta''_{k,c} \leq 1$, $k \in \mathbb{K}$.

Accordingly, if $K' = K$, $\mathbb{S}''$ is an optimal solution for (11) with $K' \leq C''_{VS} \leq K$, i.e., $C''_{VS} = K$, and $\sum_{k=1}^{K} \eta''_{k,c} = 1$, $c \in \mathbb{C}''$, $\sum_{c=1}^{C''_{VS}} \eta''_{k,c} = 1$, $k \in \mathbb{K}$.

APPENDIX C
PROOF OF THEOREM 2

It can be seen from the problem formulation in (11) that the scheduling of the V2S links and that of the U2V and V2V links are coupled together through $\underline{\mathcal{R}}_{n_2,k}$ given by (7)–(9). It is known from (7)–(9) that when $C_{V2S}, \delta_{n_1,c}, \eta_{k,c}$, $n_1 \in \mathbb{N}_1$, $k \in \mathbb{K}, c \in \mathbb{C}$, are fixed, $\underline{\mathcal{R}}_{n_2,k}$ are fixed accordingly. Thus, with fixed $C_{V2S}, \delta_{n_1,c}, \eta_{k,c}$, the scheduling of the V2S links and that of the U2V and the V2V links can be implemented independently, to respectively minimize $\sum_{n_1=1}^{N_1} p_{n_1}^{(v)} \sum_{k=1}^{K} \tau_{n_1,k}$ and $\sum_{n_2=N_1+1}^{N_1+N_2} p_{n_2}^{(uv)} \sum_{k=1}^{K} \tau_{n_2,k}$ in E_{total}.

It is straightforward that $\sum_{n_1=1}^{N_1} p_{n_1}^{(v)} \sum_{k=1}^{K} \tau_{n_1,k}$ is minimized when equality holds in (11b). Further,

$$\sum_{n_1=1}^{N_1} p_{n_1}^{(v)} \sum_{k=1}^{K} \tau_{n_1,k} \geq \sum_{n_1=1}^{N_1} p_{n_1}^{(v)} \sum_{k \in \mathfrak{k}_{n_1}} \tau_{n_1,k} \tag{36a}$$

$$= \sum_{n_1=1}^{N_1} p_{n_1}^{(v)} \frac{V_{n_1}^{QoS}}{\mathcal{R}_{n_1}}, \tag{36b}$$

and the equality in (36a) holds when $\tau_{n_1,k} = 0$, $k \notin \mathfrak{k}_{n_1}$. Thus, any group of $\tau_{n_1,k}$ satisfying (17) are optimal for the minimization of the energy consumption.

With fixed C_{V2S}, $\delta_{n_1,c}$, and $\eta_{k,c}$, the optimal scheduling of the U2V and V2V links can be obtained by solving

$$\min_{\{\tau_{n_2,k}\}} \sum_{n_2=N_1+1}^{N_1+N_2} p_{n_2}^{(uv)} \sum_{k=1}^{K} \tau_{n_2,k} \tag{37a}$$

$$s.t. \sum_{k=1}^{K} \theta_{k,n_2} \underline{\mathcal{R}}_{n_2,k} \tau_{n_2,k} \geq V_{n_2}^{QoS}, n_2 \in \mathbb{N}_2, \tag{37b}$$

$$\sum_{k=1}^{K} \tau_{n_2,k} \leq T, \sum_{n_2=N_1+1}^{N_1+N_2} \tau_{n_2,k} \leq T, n_2 \in \mathbb{N}_2, k \in \mathbb{K}, \tag{37c}$$

$$\tau_{n_2,k} \geq 0, \forall n_2, k. \tag{37d}$$

Note that for any θ_{k,n_2}, $\tau_{n_2,k}$, $\forall n_2, k$, that are optimal for (37), if we reset $\hat{\theta}_{k,n_2}$ as $\hat{\theta}_{k,n_2} = 1$ if $\tau_{n_2,k} > 0$ and $\hat{\theta}_{k,n_2} = 0$ if $\tau_{n_2,k} = 0$, the obtained $\hat{\theta}_{k,n_2}$, $\tau_{n_2,k}$, $\forall n_2, k$, are also optimal for (37). Thus, for any fixed $C_{V2S}, \delta_{n_1,c}, \eta_{k,c}$, $n_1 \in \mathbb{N}_1$, $k \in \mathbb{K}, c \in \mathbb{C}$, the optimal θ_{k,n_2} and $\tau_{n_2,k}$ can be derived based on (18) and (19). Besides, (18) is a linear programming problem as the target and the constraints in it are all linear [39].

REFERENCES

[1] C.-X. Wang, X. You, X. Gao, et al., "On the road to 6G: Visions, requirements, key technologies and testbeds," *IEEE Communications Surveys & Tutorials*, vol. 25, no. 2, pp. 905–974, Feb. 2023.

[2] Radio Communication Sector of International Telecommunication Union (ITU-R), "Future technology trends of terrestrial International Mobile Telecommunications systems towards 2030 and beyond," *Report ITU-R M.2516-0*, Nov. 2022.

[3] W. Feng, Y. Wang, Y. Chen, N. Ge, and C.-X. Wang, "Structured Satellite-UAV-Terrestrial Networks for 6G Internet of Things," *IEEE Network*, doi: 10.1109/MNET.2024.3380052, 2024.

[4] H. Saarnisaari, S. Dixit, M.-S. Alouini, et. al., "A 6G white paper on connectivity for remote areas," *6G Flagship White Papers*, arXiv:2004.14699, 2020.

[5] M.-T. Zhou, V. D. Hoang, H. Harada, J. S. Pathmasuntharam, H. Wang, P.-Y. Kong, C.-W. Ang, Y. Ge, and S. Wen, "TRITON: high-speed maritime wireless mesh network," *IEEE Wireless Communications*, vol. 20, no. 5, pp. 134–142, Oct. 2013.

[6] N. Nomikos, P. K. Gkonis, P. S. Bithas, and P. Trakadas, "A survey on UAV-aided maritime communications: deployment considerations, applications, and future challenges," *IEEE Open Journal of the Communications Society*, vol. 4, pp. 56–78, Nov. 2022.

[7] G. MARAL, M. Bousquet, and Z. Sun, "Satellite communications systems: systems, techniques and technology–sixth edition", *John Wiley & Sons, Ltd*, 2020.

[8] G. Varrall, "5G and satellite spectrum, standards, and scale", *Artech House*, 2018.

[9] Z. Lin, H. Niu, K. An, Y. Wang, G. Zheng, S. Chatzinotas, and Y. Hu, "Refracting RIS aided hybrid satellite-terrestrial relay networks: joint beamforming design and optimization," *IEEE Transactions on Aerospace and Electronic Systems*, vol. 58, no. 4, pp. 3717–3724, Aug. 2022.

[10] Z. Lin, M. Lin, B. Champagne, W.-P. Zhu, and N. Al-Dhahir, "Secrecy-energy efficient hybrid beamforming for satellite-terrestrial integrated networks," *IEEE Transactions on Communications*, vol. 69, no. 9, pp. 6345–6360, Sep. 2021.

[11] Z. Lin, M. Lin, T. de Cola, J.-B. Wang, W.-P. Zhu, and J. Cheng, "Supporting IoT with rate-splitting multiple access in satellite and aerial-integrated networks," *IEEE Internet of Things Journal*, vol. 8, no. 14, pp. 11123–11134, Jul. 2021.

[12] X. Li, W. Feng, Y. Chen, C.-X. Wang, and N. Ge, "Maritime coverage enhancement using UAVs coordinated with hybrid satellite-terrestrial networks," *IEEE Transactions on Communications*, vol. 68, no. 4, pp. 2355–2369, Apr. 2020.

[13] T. Wei, W. Feng, Y. Chen, C.-X. Wang, N. Ge, and J. Lu, "Hybrid satellite-terrestrial communication networks for the maritime Internet of Things: key technologies, opportunities, and challenges," *IEEE Internet Things J.*, vol. 8, no. 11, pp. 8910–8934, Jun. 2021.

[14] Y. Wang, W. Feng, J. Wang, and T. Q. S. Quek, "Hybrid satellite-UAV-terrestrial networks for 6G ubiquitous coverage: a maritime communications perspective," *IEEE Journal on Selected Areas in Communications*, vol. 39, no. 11, pp. 3475–3490, Nov. 2021.

[15] W. Feng, Y. Lin, Y. Wang, J. Wang, Y. Chen, N. Ge, S. Jin, and H. Zhu, "Radio map-based cognitive satellite-UAV networks towards 6G on-demand coverage," *IEEE Transactions on Cognitive Communications and Networking*, doi: 10.1109/TCCN.2023.3345857, Dec. 2023.

[16] Y. Wang, and Z. Lu, "Coordinated resource allocation for satellite-terrestrial coexistence based on radio maps," *China Communications*, Vol. 15, No. 3, pp. 149–156, Mar. 2018.

[17] T. M. Braun and W. R. Braun, "Satellite communications payload and system," *John Wiley & Sons, Inc.*, 2021.

[18] M. Tropea, P. Fazio, F. De Rango, and A. F. Santamaria, "Novel MF-TDMA/SCPC switching algorithm for DVB-RCS/RCS2 return link in railway scenario," *IEEE Transactions on Aerospace and Electronic Systems*, vol. 52, no. 1, pp. 275–287, Feb. 2016.

[19] W. Kogler, H. Schlemmer, and O. Koudelka, "Timing synchronization in MF-TDMA systems for geostationary satellites," *IEEE Communications Magazine*, vol. 45, no. 12, pp. 36–42, Dec. 2007.

[20] E. Lagunas, S. K. Sharma, S. Maleki, S. Chatzinotas, and B. Ottersten, "Resource allocation for cognitive satellite communications with incumbent terrestrial networks," *IEEE Transactions on Cognitive Communications and Networking*, vol. 1, no. 3, Sept. 2015.

[21] P. K. Sharma, P. K. Upadhyay, D. B. da Costa, P. S. Bithas, and A. G. Kanatas, "Performance analysis of overlay spectrum sharing in hybrid satellite-terrestrial systems with secondary network selection," *IEEE Transactions on Wireless Communications*, vol. 16, no. 10, pp. 6586–6601, Oct. 2017.

[22] Z. Lin, M. Lin, J. Wang, T. Cola, and J. Wang, "Joint beamforming and power allocation for satellite-terrestrial integrated networks with non-Orthogonal multiple access," *IEEE Journal of Selected Topics in Signal Processing*, vol. 13, no. 3, pp. 657–670, Jun. 2019.

[23] F. Pervez, L. Zhao, and C. Yang, "Joint user association, power optimization and trajectory control in an integrated satellite-aerial-terrestrial network," *IEEE Transactions on Wireless Communications*, vol. 21, no. 5, pp. 3279–3290, May 2022.

[24] L. You, K. -X. Li, J. Wang, X. Gao, X. -G. Xia, and B. Ottersten, "Massive MIMO transmission for LEO satellite communications," *IEEE Journal on Selected Areas in Communications*, vol. 38, no. 8, pp. 1851–1865, Aug. 2020.

[25] M. A. Clark, and K. Psounis, "Equal interference power allocation for efficient shared spectrum resource scheduling," *IEEE Transactions on Wireless Communications*, Vol. 16, No. 1, pp. 58–72, Jan 2017.

[26] M. Höyhtyä, A. Mämmelä, X. Chen, A. Hulkkonen, J. Janhunen, J. Dunat, and J. Gardey, "Database-assisted spectrum sharing in satellite communications: a survey," *IEEE Access*, vol. 5, pp. 25322–25341, Nov. 2017.

[27] Y. Ruan, Y. Li, C.-X. Wang, R. Zhang, and H. Zhang, "Energy efficient power allocation for delay constrained cognitive satellite terrestrial networks under interference constraints," *IEEE Transactions on Wireless Communications*, vol. 18, no. 10, pp. 4957–4969, Oct. 2019.

[28] S. R. Saunders, A. Aragon-Zavala, "Antennas and propagation for wireless communication systems – second edition," *John Wiley & Sons, Ltd*, 2007.

[29] G. E. Corazza and F. Vatalaro, "A statistical model for land mobile satellite channels and its application to nongeostationary orbit systems," *IEEE Transactions on Vehicular Technology*, vol. 43, no. 3, pp. 738–742, Aug. 1994.

[30] A. Abdi, W. C. Lau, M.-S. Alouini, and M. Kaveh, "A new simple model for land mobile satellite channels: first- and second-order statistics," *IEEE Transactions on Wireless Communications*, vol. 2, no. 3, pp. 519–528, May 2003.

[31] Radio Communication Sector of International Telecommunication Union (ITU-R), "Propagation data required for the design of earth-space land mobile telecommunication systems", *Recommendation ITU-R P.681-6*, 2019.

[32] A. Al-Hourani, S. Kandeepan, and S. Lardner, "Optimal LAP altitude for maximum coverage," *IEEE Wireless Communications Letters*, vol. 3, no. 6, pp. 569–572, Dec. 2014.

[33] S. Jo and W. Shim, "LTE-maritime: high-speed maritime wireless communication based on LTE technology," *IEEE Access*, vol. 7, pp. 53172–53181, 2019.

[34] C.-X. Wang, J. Huang, H. Wang, X.-Q. Gao, X.-H. You, and Y. Hao, "6G wireless channel measurements and models: trends and challenges," *IEEE Veh. Technol. Mag.*, vol. 15, no. 4, pp. 22—32, Dec. 2020.

[35] C.-X. Wang, Z. Lv, X. Gao, X.-H. You, Y. Hao, and H. Haas, "Pervasive wireless channel modeling theory and applications to 6G GBSMs for all frequency bands and all scenarios," *IEEE Trans. Veh. Technol.*, vol. 71, no. 9, pp. 9159—9173, Sept. 2022.

[36] K.-X. Li, X.-Q. Gao, and X.-G. Xia, "Channel estimation for LEO satellite massive MIMO OFDM communications," *IEEE Transactions on Wireless Communications*, vol. 22, no. 11, pp. 7537–7550, Nov. 2023.

[37] J. Lee and S. Leyffer, "Mixed integer nonlinear programming," *Springer Science+Business Media, LLC*, 2012.

[38] W. Feng, Y. Wang, D. Lin, N. Ge, J. Lu, and S. Li, "When mmWave communications meet network densification: a scalable interference coordination perspective," *IEEE Journal on Selected Areas in Communications*, vol. 35, no. 7, pp. 1459-1471, Jul. 2017.

[39] G. B. Dantzig, "Linear programming and extensions," *Princeton University Express*, 1998.

[40] S. Axler, "Linear algebra done right – third edition," *Springer International Publishing*, 2014.

[41] G. James, D. Witten, T. Hastie, and R. Tibshirani, "An introduction to statistical learning," *Springer Berlin Heid*, 2022.

[42] I.-S. Koh, T. Hwang, "Simple expression of ergodic capacity for Rician fading channel," *IEICE Transactions on Communications*, vol.93, no. 6, pp. 1594-1596, 2010.

[43] Radio Communication Sector of International Telecommunication Union (ITU-R), "Reference radiation pattern for earth station antennas in the fixed-satellite service for use in coordination and interference assessment in the frequency range from 2 to 31 GHz," *Recommendation ITU-R S.465-6*, 2010.